



OPEN ACCESS

EDITED BY

Anne C. Moore,
University College Cork, Ireland

REVIEWED BY

Nahid Ali,
Indian Institute of Chemical Biology
(CSIR), India
Rachel Yoon Chang,
The University of Sydney, Australia

*CORRESPONDENCE

Aneesh Thakur,
aneesh.thakur@sund.ku.dk
Camilla Foged,
camilla.foged@sund.ku.dk

†PRESENT ADDRESS

Guillermo Cano-Garcia,
Alk Abelló, Madrid, Spain
Fabrice Rose,
ZICCUM AB, Lund, Sweden
Peter Andersen,
Novo Nordisk Foundation, Hellerup,
Denmark

SPECIALTY SECTION

This article was submitted to Vaccine
Delivery,
a section of the journal
Frontiers in Drug Delivery

RECEIVED 20 June 2022

ACCEPTED 28 July 2022

PUBLISHED 07 September 2022

CITATION

Thakur A, Xu Y, Cano-Garcia G, Feng S,
Rose F, Gerde P, Andersen P,
Christensen D and Foged C (2022),
Optimizing the design and dosing of dry
powder inhaler formulations of the
cationic liposome adjuvant CAF@01 for
pulmonary immunization.
Front. Drug. Deliv. 2:973599.
doi: 10.3389/fddev.2022.973599

COPYRIGHT

© 2022 Thakur, Xu, Cano-Garcia, Feng,
Rose, Gerde, Andersen, Christensen and
Foged. This is an open-access article
distributed under the terms of the
[Creative Commons Attribution License
\(CC BY\)](https://creativecommons.org/licenses/by/4.0/). The use, distribution or
reproduction in other forums is
permitted, provided the original
author(s) and the copyright owner(s) are
credited and that the original
publication in this journal is cited, in
accordance with accepted academic
practice. No use, distribution or
reproduction is permitted which does
not comply with these terms.

Optimizing the design and dosing of dry powder inhaler formulations of the cationic liposome adjuvant CAF@01 for pulmonary immunization

Aneesh Thakur^{1*}, You Xu¹, Guillermo Cano-Garcia^{1†}, Siqi Feng¹,
Fabrice Rose^{1†}, Per Gerde^{2,3}, Peter Andersen^{4†},
Dennis Christensen⁴ and Camilla Foged^{1*}

¹Department of Pharmacy, Faculty of Health and Medical Sciences, University of Copenhagen, Copenhagen, Denmark, ²Inhalation Sciences Sweden AB, Huddinge, Sweden, ³Institute of Environmental Medicine, Karolinska Institutet, Stockholm, Sweden, ⁴Department of Infectious Disease Immunology, Statens Serum Institut, Copenhagen, Denmark

Thermostability is one of the product characteristics preferred by WHO for vaccines against respiratory infections due to ease of administration, pain minimization, and low costs. Thermostable dry powder inhaler (DPI) vaccine formulations can induce protective antibodies and T cells at the site of infection in the lungs. However, the majority of licensed human vaccines is based on liquid dosage forms, and there is no licensed mucosal adjuvants. The cationic adjuvant formulation 01 (CAF@01) is a liposome-based adjuvant system that (i) induces robust T cells and antibodies, (ii) is safe and well-tolerated in clinical trials, and (iii) induces mucosal immune responses after pulmonary administration. However, the optimal DPI formulations of CAF@01 for pulmonary immunization are not known. Here, we show that DPI formulations of CAF@01 spray-dried with a combination of sugars and the amino acid leucine exhibit optimal aerosolization properties and distribute in the lung lobes upon pulmonary administration. We demonstrate that the type of amorphous sugar used as stabilizer and the amount (w/w) of leucine used during spray drying affect the physicochemical properties and aerosol performance of DPI formulations. By systematically varying the ratios (w/w) of trehalose, dextran and leucine used as excipients during spray drying, we manufactured DPI formulations of CAF@01 that displayed (i) a spherical or wrinkled surface morphology, (ii) an aerodynamic diameter and particle size distribution optimal for deep lung deposition, and (iii) solid-state and aerosolization properties suitable for lung delivery. Using a design-of-experiments-based approach, we identified the most optimal process parameters in an *in vivo* aerosol generator, *i.e.*, the PreciseInhale® system, which was used to measure the flowability of the aerosols. We found that the DPI formulation of CAF@01 spray-dried with trehalose and dextran (70% w/w) and leucine (30% w/w) displayed the most optimal physicochemical, morphological, solid-state, and aerosolization properties for deep lung deposition. Upon pulmonary administration, this DPI formulation distributed

in the lung lobes in a way that was almost identical to the biodistribution of the non-spray dried formulation. Hence, DPI formulations of CAF@01, prepared with trehalose and dextran sugar matrix and a leucine shell, display physicochemical and aerosol properties suitable for inhalation.

KEYWORDS

CAF@01, spray—drying, design of experiments (DOE), pulmonary administration, dry powders, biodistribution

Introduction

Vaccines represent the cornerstone of global public health care (Remy et al., 2015). The development of safe and efficacious vaccines against respiratory infectious diseases, e.g., tuberculosis (TB), influenza, and coronaviruses, remains a global challenge. Among the current vaccine platforms, the recombinant subunit protein technology is highly safe, but subunit antigens are often poorly immunogenic, and require adjuvants to enhance the induction of protective immune responses (Del Giudice et al., 2018). Despite a major research effort, only few adjuvants have been approved for human prophylactic vaccines, and none of them is used for mucosal immunization (Iwasaki and Omer, 2020). Therefore, the development of adjuvants that can be used for subunit vaccines in the respiratory mucosa is a medical necessity.

The design of dry powder inhaler (DPI) formulations of vaccines is one of the World Health Organization's preferred product characteristics for vaccines against several respiratory infections, e.g., TB (Schrager et al., 2018), influenza (Neuzil et al., 2017), and COVID-19 (WHO, 2022). WHO encourages innovations aimed at improving programmatic suitability in the field of thermostability, ease of delivery, and pain minimization. This is based on the rationale that vaccines based on DPI formulations can (i) eliminate the need for the cold chain, which will reduce the overall vaccine costs, (ii) increase the availability of the product, which is crucial in low- and middle-income countries that lack sufficient infrastructure and resources, and (iii) be self-administered, which can improve patient compliance and safety of vaccine administration. In addition, the vaccines administered into the lungs have the capability to train innate immune cells (Vierboom et al., 2021), and induce tissue-resident memory cells (Perdomo et al., 2016) and protective secretory IgA antibodies (Lapuente et al., 2021).

DPI formulations of vaccines can be prepared using a number of different drying methods (Ghaemmaghamian et al., 2022). Spray drying is one such method, which is a continuous and rapid manufacturing process to produce DPI formulations. Unlike other drying methods, one of the distinct advantages of spray drying is the scope to engineer the physicochemical and solid-state properties of the DPI formulations to present aerodynamic properties suitable for deep lung deposition (Vehring, 2008; Sou et al., 2011). Spray drying is a mild

drying process for subunit protein antigens and has been applied for manufacturing several recombinant-based subunit protein vaccines (Gomez and Vehring, 2022). Drying in the presence of stabilizers, e.g., sugars, is one of the proven strategies used to protect proteins and nanoparticles during drying and in the solid state (Wang, 2000; Lokras et al., 2021). Several theories have been propounded on the stabilization of proteins and nanoparticles by sugars including the classical vitrification (immobilization of particles in a rigid, amorphous glassy sugar matrix) and water replacement (replacing hydrogen bonds between water and the particles) theories (Mensink et al., 2017). However, mere adding any sugar to a protein/particle and drying does not promise protein/particle stabilization, as not all sugars are equally efficient as stabilizers. Therefore, to facilitate stabilization, the choice of sugar and drying method are of utmost importance. Amino acids are also used as stabilizers for biomolecule formulations, and they stabilize proteins/particles by direct binding to protein molecules via hydrogen bonding or ion–dipole interactions (Ajmera and Scherliess, 2014).

The cationic adjuvant formulation 01 (CAF@01) is a liposome-based adjuvant system that is composed of the cationic lipid dimethyldioctadecylammonium (DDA) bromide and the glycolipid immunopotentiator trehalose 6,6'-dibehenate (TDB) (Davidsen et al., 2005). CAF@01 liposomes induce cell-mediated immune (CMI) responses characterized by a strong CD4⁺ Th1/Th17 profile and humoral responses (Davidsen et al., 2005; van Dissel et al., 2014). Consequently, CAF@01 is an attractive adjuvant system for vaccine candidates to prevent diseases that require highly complex immune responses, i.e., antibodies and CMI responses such as influenza, malaria, AIDS, and TB (Davidsen et al., 2005; Agger et al., 2008). The cationic headgroup charge of DDA induces depot formation of CAF@01 at the site of injection and enhances Th1-type immune responses (Henriksen-Lacey et al., 2010). TDB provides colloidal stability to the cationic DDA liposomes and binds to the C-type lectin receptor Mincle, which activates a signaling cascade, leading to increased macrophage activation and induction of Th1/Th17-type immune responses (Werninghaus et al., 2009; Schoenen et al., 2010). CAF@01 has been tested preclinically with different vaccine antigens (Fomsgaard et al., 2011; Christensen et al., 2017; Wern et al., 2017) and was found to be safe, well-tolerated, and immunogenic in phase I clinical trials (Roman et al., 2013;

Abraham et al., 2019; Dejon-Agobe et al., 2019). Recently, we have demonstrated the potential of CAF@01 to induce immune responses at the mucosal surfaces in the lungs following pulmonary immunization (Thakur et al., 2018a). We have shown that DPI formulations of CAF@01 prepared using spray drying retain their adjuvanticity following parenteral administration similar to the liquid formulation (Ingvarsson et al., 2013a). We also demonstrated that a DPI formulation of the TB subunit fusion protein antigen H56 adjuvanted with CAF@01 displayed similar immunogenicity as the non-spray dried vaccine formulation following parenteral administration (Thakur et al., 2018b).

With the long-term objectives to develop a self-administrable, thermostable TB vaccine and to exploit the mucosal adjuvant effect of CAF@01, we manufactured DPI formulations of CAF@01 without H56 antigen using spray drying, and we tested trehalose, mannitol, dextran and leucine as stabilizing excipients. The resulting DPI formulations were thoroughly characterized with respect to physicochemical properties, morphology, solid state, and aerosolization properties. Using a quality-by-design (QbD) approach, we identified process parameters in the PreciseInhale® (PI) system that can be used for *in vivo* delivery of respiratory aerosols. Finally, we examined the lung uptake and distribution of the most optimal DPI formulation of CAF@01 following pulmonary administration. We found that the DPI formulation of CAF@01, spray-dried in the presence of a specific weight ratio of trehalose, dextran, and leucine, displayed the most optimal aerosolization properties and was distributed in the lung lobes in a way that was almost identical to the biodistribution of the non-spray dried formulation. These findings indicate that DPI formulations of CAF@01 can be further exploited as solid dosage forms for delivering subunit protein antigens to the lungs.

Materials and methods

Materials

DDA was obtained from Avanti Polar Lipids (Alabaster, AL, United States). TDB was purchased from Niels Clauson-Kaas A/S (Farum, Denmark). Mannitol, trehalose dihydrate, and L-leucine were purchased from Sigma-Aldrich (St. Louis, MO, United States), while dextran (6 kDa) was obtained from Alfa Aesar (Haverhill, MA, United States). Xenolight™ 1,10-dioctadecyl-3,3,30,30-tetramethylindotricarbocyanine iodide (DiR) near infra-red fluorescent dye was purchased from Perkin Elmer (Waltham, MA, United States). The PreciseInhale® dispensing system containing an active aerosol dosing system integrated into the exposure control program was used to examine the aerosol performance of the powders and was obtained from Inhalation Sciences Sweden AB (Huddinge,

Sweden). The PreciseInhale® system includes the data logging instrument CEL-712 Microdust Pro Real-time Dust Monitor (Casella, Bedford, United Kingdom), which displays real-time graphical dust levels. Water was prepared with a Millipore Direct-Q3 UV system (Billerica, MA, United States). All other chemicals and reagents were of analytical grade and were acquired from commercial suppliers.

Preparation of CAF@01 liposomes

Liposomes were prepared using the thin film method as previously described (Davidsen et al., 2005). Briefly, weighed amounts of DDA and TDB (5:1, w/w) were dissolved in chloroform/methanol (9:1, v/v) in a round bottom flask. The organic solvents were removed by rotary evaporation (Laborota 4011 digital, Heidolph Instruments, Schwabach, Germany) under vacuum after cleaning twice with 99% (v/v) ethanol resulting in the formation of a thin lipid film. The lipid film was rehydrated in Milli-Q water containing 18 mg/ml trehalose (T), dextran (D), or mannitol (M), or a mixture of these sugars at different ratios. The lipid film was bath-sonicated for 5 min using an ultrasound cleaner (Branson Ultrasonic Cleaner, Danbury, CT, United States), and heated to 60 °C for 1 h in a water bath with vortexing every 10 min. At the 20th min of rehydration, the liposomes were tip-sonicated for 20 s using a MISONIX S-4000 probe sonicator (LLC, Newtown, CT, United States) (amplitude 70, power 16 W) to reduce their size and vortexed for 1 min. The liposomes were annealed for 1 h at room temperature. The final concentration of CAF@01 was 1.67/0.33 mg/ml of DDA/TDB, corresponding to a molar ratio of 89:11. Fluorescently labeled CAF@01 was prepared by addition of Xenolight™ DiR dissolved in ethanol during the preparation of the lipid film, resulting in a DiR concentration of 0.025 mg/ml in the final formulation.

Spray drying

Liposome dispersions were spray-dried with a co-current Büchi B-290 mini spray dryer (Büchi Labortechnik, Flawil, Switzerland) equipped with a two-fluid nozzle with an orifice diameter of 0.7 mm using nitrogen as the atomization gas. Trehalose, mannitol, or dextran, or mixtures of these sugars with leucine at different weight ratios, were used as stabilizing excipient. The dry powder particles were separated from the airstream by centrifugal forces using a high-performance cyclone (Büchi Labortechnik). The feedstock concentration was 20 mg/ml (2 mg/ml DDA/TDB). Spray drying was performed at a feed flow rate of 1.5 ml/min, an inlet temperature of approximately 82 °C, an outlet temperature of 50 °C, an aspirator capacity of 90%, and an atomizing airflow of 414 L/h. These spray drying conditions were previously optimized using a QbD approach in the lab (data not published) and were used in our recent work

with interfering RNA (siRNA) containing nanoparticles (Xu et al., 2022a). To prepare DPI microparticles with different sizes, atomizing airflows of 414, 473, 536, 601, 670, or 742 L/h were used. The resulting powders were stored in a desiccator over a silica gel at 4 °C.

Size, polydispersity index, and zeta potential

Liquid (non-spray-dried) and DPI CAF®01 formulations, reconstituted to 20 mg/ml with Milli-Q water, were characterized with respect to average intensity-weighted hydrodynamic diameter (*z*-average) and polydispersity index (PDI) by dynamic light scattering using a Zetasizer Nano ZS (Malvern Instruments, Worcestershire United Kingdom) equipped with a 633 nm laser and 173° detection optics. Malvern Zetasizer software v6.20 (Malvern Instruments) was used for data acquisition. The DPI formulations were diluted 10-fold in Milli-Q water, except for the powders containing dextran, which were diluted 50-fold. The surface charge of liquid (non-spray-dried) and reconstituted DPI CAF®01 formulations was estimated by analysis of the zeta potential using laser-Doppler micro-electrophoresis. The non-spray-dried samples were diluted 100-fold in 10 mM Tris buffer (pH 7.4), and the DPI formulations were diluted to 18 mg/ml solution of trehalose and dextran. All measurements of size, PDI, and zeta potential were repeated three times for each sample.

Dry powder yield

The dry powder yield of the spray drying process was measured as the weight difference in the collected powder, compared to the initial total solid content of the dispersions before spray drying. It was calculated as the weight difference of the collection vial before and after spray drying, divided by the initial total solid content of the dispersions (Equation 1).

$$\text{Yield (\%)} = \frac{\text{Wt. of vial after spray drying (mg)} - \text{Wt. of vial before drying (mg)}}{\text{Initial total solid content (mg)}} \times 100\% \quad (1)$$

Moisture, aerodynamic particle size, and morphology

The residual powder moisture content was determined by thermogravimetric analysis (TGA) after heating approximately 10 mg sample at a constant rate of 30 °C/min up to 300 °C using a Discovery TGA 550 (Perkin Elmer, Waltham, MA, United States) with nitrogen purging. The selection of these temperature and ramp conditions is based on a previously

established protocol in the lab (Lokras et al., 2021) that has been used in our recent study with siRNA-loaded nanoparticles (Xu et al., 2022a). The data was analysed using the TRIOS program (TA Instruments, New Castle, DE, United States). The water loss caused by water evaporation was calculated in percent and defined as the moisture content. The aerodynamic particle size was measured using an Aerodynamic Particle Sizer (APS) Spectrometer® 3321 equipped with a Small-Scale Powder Disperser® (both TSI, Shoreview, MN, United States) to generate the aerosol, as described previously (Ingvarsson et al., 2013a). The Aerosol Instrument Manager® Software, Version 8.1.0.0 (TSI), was used to convert the resulting particle size distribution into mass median aerodynamic diameter (MMAD). The morphology of the DPI CAF®01 formulations was examined by scanning electron microscopy (SEM) using a Hitachi TM3030 SEM (Chiyoda, Japan) operated at an accelerating voltage of 15 kV, a working distance of 5.8 mm, and an emission current of 53.5 A. The magnification was set at ×2000. Prior to imaging, the DPI formulations were sprinkled onto a stub covered with double-adhesive carbon tape, and sputter coated with gold at a current supply of 30 mA for 30 s using a Cressington Sputter Coater 108 (Cressington Scientific Instruments, Watford, United Kingdom). SEM images were also analyzed to determine the particle size using the ImageJ software.

Aerosol exposure using the Preciselnhale® system

The PI system was used to generate the aerosols, as previously described (Gerde et al., 2004; Selg et al., 2013; Malmlof et al., 2019). The DPI loading in the PI system, aerosol generation, and gravimetric analysis of the aerosols were performed as described recently in detail (Xu et al., 2022a). For the pre-DoE optimization studies, the following parameters were used: an impactor nozzle was used for aerosol exposures, a superimposed flow rate of 400 ml/min, an aerosol generation pressure of 120 bar, a main valve reset pressure of 40 bar, a pre-exposure aerosol mixing period of 0.6 s, and a pressure chamber volume displacement of 4 mm. During aerosol generation, 1 mg DPI formulation was loaded into the retractable powder chamber bottom, inserted into the PI system, and secured. The exposure time of the powders was 90 s. The purpose of the aerosol generation procedure was to test the flowability of the powders, which was measured as the Casella maximum concentration (C_{\max}). The amount of aerosol likely to be deposited onto the inhalation filter (M_{cas}), and the C_{\max} of each DPI formulation, was measured five times using the Casella Microdust Pro Monitor that displays the real-time graphical dust or aerosol levels. We varied systematically: (i) the generation pressure, (ii) the main valve reset pressure, and (iii) the pressure chamber volume displacement, to identify the optimal process parameters resulting in the highest C_{\max} and

TABLE 1 Process design space.

Factor	Low level	Centre level	High level
Generation pressure (bar)	100	130	160
Reset pressure (bar)	40	65	90
Plunger displacement (mm)	2.0	4.5	7.0

M_{cas} . For aerosolization of TiO_2 (Sigma-Aldrich), which was used as the reference powder (positive control), a decompression nozzle was used, because it is suitable for more loosely packed powders. For TiO_2 , the generation pressure was decreased to 100 bar, and the pressure chamber volume displacement was increased to 7 mm.

Dry powder aerosol yield in the Preciselnhale® system

The percentage of dry powder deposited in the end filter, placed on the exposure block after PI system exposure of the DPI formulations, was measured to determine the aerosol yield. It was calculated as the weight difference of the end filter before and after PI exposure of the DPI formulations, divided by the weight of the powder loaded in the powder chamber (Equation 2). Five measurements for each condition were performed to calculate the aerosol yield.

$$\text{Aerosol yield \%} = \frac{\text{End filter after exposure (mg)} - \text{End filter before exposure (mg)}}{\text{Powder weight loaded in the powder chamber (mg)}} \times 100\% \quad (2)$$

The quality-by-design process: Experimental design

A QbD approach applying design of experiments (DoE) was used to identify the optimal process parameters (operator settings) of the PI system to achieve maximal flowability (C_{max}) of DPI CAF@01-trehalose/dextran (T/D) formulations. We defined the optimal design space by identifying critical process parameters (Table 1) and critical quality attributes (Table 2) in the dry powder aerosolization process in the PI system. Subsequently, the experiment was designed and set up using MODDE 12.0 (Umetrics AB, Umeå, Sweden). Three

factors, *i.e.*, (i) the generation pressure, (ii) the reset pressure, and (iii) the plunger displacement, were varied at low, centre and high levels, respectively (Table 1). These process parameters in the PI system control the aerosolization of the powders into the holding chamber. Two responses, *i.e.*, the C_{max} and the ejected volume, were measured as critical quality attributes, as defined in the quality target product profile (QTPP) for the performance of the DPI formulations in the PI system (Table 2). A higher C_{max} value in the Casella Microdust Pro monitor reflects a high flowability of the powders. The ejected volume is the volume of air required for aerosol generation, and it should preferably be in the range of 70–95 ml for aerosol deposition in murine animal models according to the manufacturers of the PI system. A central composite face (CCF) centered fractional factorial design was chosen to explore the effects of the primary, secondary and interactional terms (Supplementary Figure S1). A total of 17 experimental runs were conducted (referred to as N1–N17, Supplementary Table S1), of which eight represented a two-level fractional factorial design (Werninghaus et al., 2009), three experimental runs were center points, and six experiments were star points. Each experiment was repeated six times. Subsequently, the optimal operating space was defined.

Particle deposition measured using a multi-stage impactor system

The *ex vivo* lung deposition behaviour of the DPI formulations loaded into a clinical inhaler device was investigated using the Next Generation Pharmaceutical Impactor (NGI, Copley Scientific, Nottingham, United Kingdom) with a mouth piece adapter and an induction throat (USP throat). An equivalent amount of 20 ± 1.0 mg DPI formulation was loaded manually in a size 3 capsule (Capsugel, Bornem, Belgium) and dispersed through an Aerolizer® dry powder inhaler (Novartis, Basel, Switzerland). A standard pharmacopeia dispersion procedure was used (USP 39 <601>), whereby 4 L air was passed through the inhaler at an airflow rate of 100 L/min for 2.4 s, with a pressure drop of approximately 4 kPa across the device. Aerosol particles were collected onto 1.6 μ m pore size glass fiber filters Grade GF/A (Whatman, Fisher Scientific, United Kingdom) in each stage. The samples were analyzed in triplicate. The fine particle fraction (FPF%) and the emitted dose (ED%) were calculated according to Equations 3, 4:

TABLE 2 Quality target product profile (QTPP) for the performance of dry powder inhaler formulations of CAF@01 liposomes in the Preciselnhale® system.

Response	Target	Reason
Casella maximum concentration (C_{max}) (mg/ml)	5.5	Higher C_{max} reflects higher flowability of the powder formulation
Ejected volume (ml)	90	Important for <i>in vivo</i> experiments

$$\text{FPF}\% = \frac{\text{Fine particle dose (less than 3.42 } \mu\text{m)}}{\text{Initial mass in capsule}} \times 100\% \quad (3)$$

$$\text{ED}\% = \frac{\text{Initial mass in capsule} - \text{Final mass remaining in capsule}}{\text{Initial mass in capsule}} \times 100\% \quad (4)$$

X-ray powder diffraction

Based on the optimal process parameters (operator settings) in the PI system identified using DoE, the DPI CAF@01-Trehalose/Dextran formulations (CAF@01-T/D 30:70) with and without leucine were characterized for powder diffraction patterns. The X-ray powder diffraction (XRPD) patterns were recorded with a PANalytical X-ray diffractometer of the XPERT PRO type with a PW 3050/60 generator and a PIXcel Detector (PANalytical, Almelo, Netherlands). The X-ray diffractometer was operated with an anode current of 40 mA and an accelerating voltage of 30 kV. The samples were gently deposited onto an aluminium sample tray and exposed to a CuK α radiation source at diffraction angles (2- θ) from 5° to 35° in a step mode using a step size of 0.02° of 2- θ and a collection time of 96 s per step. A sample rotation of 30 rpm was applied throughout the scans. For the data analysis, the X'Pert Data Collector software for automatic powder diffraction version 2.2i (PANalytical) was used.

Differential scanning calorimetry

The thermotropic phase behaviour of the reconstituted DPI formulations of CAF@01-T and CAF@01-T/D (30:70) were determined by differential scanning calorimetry (DSC) using a nano DSC (TA Instruments). The final concentration of the liposomal dispersions was 20 mg/ml (2 mg/ml DDA/TDB). The samples were heated from 20 °C to 70 °C at a scanning rate of 0.5 °C/min. Three scans per sample were performed. For data analysis, the Origin® 7 software (OriginLab Corporation, Northampton, MA, United States) was used.

HPLC quantification of DDA

Quantification of the DDA content in the DPI formulation of CAF@01-T/D (30:70):leucine (L) was performed with in Agilent 1260 Infinity (Santa Clara, CA, United States) HPLC system using an evaporative light scattering detector (ELSD). The ELSD was configured to display nebulizer and evaporator temperatures of 50 °C and 90 °C, respectively, while the nitrogen gas flow rate was kept at 1.3 ml/min. The HPLC system was equipped with a Phenomenex Luna C18 (2) column (Torrance, CA, United States) of dimensions 150 mm \times 4.6 mm, a particle

size of 3 μ m, and a pore size of 100 Å. The samples for analysis were prepared by diluting the formulations with methanol. A volume of 30 μ L was injected, and the DDA was separated using the same column. The separation was performed at 50 °C using 0.1% (v/v) trifluoroacetic acid in water (eluent A) and methanol (eluent B) at a flow rate of 1.3 ml/min. The calibration curve for DDA (retention time 6.45 min) was linear in the investigated DDA concentration range of 15–250 μ g/ml (Supplementary Figure S6H). Data processing was carried out using the Agilent Chemstation software.

Pulmonary biodistribution of DPI formulations

Ten female 8–10 weeks old BALB/cOlaHsd mice (Envigo, Limburg, Netherlands) were housed in individually ventilated cages and allowed to acclimatize for at least 1 week upon arrival. Autoclaved water and food (standard rodent diet, Brogaarden, Lyngø, Denmark) were provided ad libitum. All experimental work was approved by the Danish National Experiment Inspectorate under permit 2016-15-0201-01026 and was performed in accordance with the European Community directive 86/609 for the care and use of laboratory animals. The diet was changed to a chlorophyll-free diet (AIN-76A, Brogaarden) at least 7 days prior to experimentation to reduce background fluorescence signal. Mice were randomly divided into two groups ($n = 5/\text{group}$), liquid and DPI CAF@01-T/D (30:70) formulation groups. For a previous radionuclide imaging experiment with H56/CAF@01, we used three mice per group (Thakur et al., 2018a). However, to increase the statistical power, here we included five mice in each group. Mice in the first group received the liquid (non-spray dried) Xenolight™ DiR-labeled CAF@01-T/D (30:70):L 70:30 formulation, while mice in the second group received the DPI Xenolight™ DiR-labeled CAF@01-T/D (30:70):L 70:30 formulation. Mice in both groups were imaged for fluorescence signal before intrapulmonary administration, immediately post-administration, and 1 h post-administration of the formulations. Mice were euthanized 1 h post-administration, and their trachea and lung lobes were collected for evaluating fluorescence signal intensity. The following parameters were assessed: the intensity of the emitted light (photons/s/cm²/steradian) from a region of interest (ROI) in the images, and the percentage of the relative dose in the trachea and the lung lobes. *In vivo* imaging was performed after intrapulmonary administration of liquid and DPI formulations of Xenolight™ DiR labelled CAF@01-T/D (30:70):L 70:30, respectively. For the liquid formulation, mice were dosed with a total volume of 50 μ L formulation, corresponding to a DDA/TDB dose of 125/25 μ g/mouse. The MicroSprayer®

Syringe Assembly (MSA-250-M, PennCentury, Wyndmoor, PA, United States) was used for pulmonary administration of liquid formulation as previously described (Thakur et al., 2018a). Briefly, mice were anesthetized by intraperitoneal injection of ketamine (MSD Animal Health, Denmark)/xylazine (Rompun Vet, Bayer, Copenhagen, Denmark) 100/5 mg/kg, respectively, and placed on a rodent tilting work stand at a 45° angle by the upper incisors (Hallowell EMC, Pittsfield, MA, United States). A cold light source with a flexible fiber-optics arm (SCHOTT AG, Mainz, Germany) was used for optimal illumination of the trachea, which appeared as a white light spot. A cotton swab was used to open the lower jaw of the mouse, and the tongue was displaced to the left with a blunted forceps. A laryngoscope (WelchAllen, Skaneateles Falls, NY, United States) fitted with a 41 mm intubation specula (Hallowell EMC) was used with the other hand for maximal oropharyngeal exposure. After a clear view of the trachea, the laryngoscope with the specula was taken out. For intrapulmonary administration, the tip of the MicroSprayer®/Syringe Assembly loaded with 50 µL formulation was gently inserted in the trachea of anesthetized animal – near to, but not touching the carina (first bifurcation), and the plunger of the assembly was pushed to aerosolize the formulation to ensure uniform administration into both lungs. The tip of the syringe was immediately withdrawn, and the mouse was taken off the intubation stand. A Dry Powder Insufflator (DP-4M; PennCentury) attached to a PennCentury Air Pump (Model AP-1) was used to intrapulmonary administer the DPI formulation to animals, as previously described (Xu et al., 2022a). The animals were anesthetized and prepared for the procedure as described above. The powder was administered using five puffs of air of 200 µL (maximum volume allowed for a mouse in one puff), generated by the air pump connected to the insufflator. The administered dose was determined by weighing the insufflator before and after the five air puffs. Approximately 1 mg DPI formulation CAF@01-T/D (30:70):L 70:30 was used for loading the insufflator per animal. The average emitted dose from the insufflator was 0.75 ± 0.13 mg powder for 1 mg powder loading (Supplementary Figure S6K). Imaging was performed immediately ($t = 0$) and 1 h after dosing using an *In Vivo* Imaging System (IVIS) Lumina XRMS imaging system (PerkinElmer, Waltham, MA, United States). During the imaging procedure, the mice were anesthetized using isoflurane (1%–3% for maintenance, up to 4% for induction) and oxygen from a precision vaporizer. Mice were euthanized 1 h post-administration using CO₂, and the lungs and the trachea were isolated. Lung tissue, either whole lungs or dissected into lung lobes, was placed into Petri dishes, and evaluated using the IVIS Lumina XRMS at an excitation wavelength of 715 nm and an emission wavelength of 745 nm. The intensity of the emitted light (photons/s/cm²/steradian) was quantified using the Living Image® Software

v4.3.1 (PerkinElmer). The distribution of the formulations was also assessed by calculating the relative percentage of the dose in the trachea and the individual lung lobes (Equation 5).

$$\text{Relative dose (\%)} = \frac{\text{Fluorescence intensity in trachea or individual lung lobes}}{\text{Total fluorescence intensity in lungs}} \times 100\% \quad (5)$$

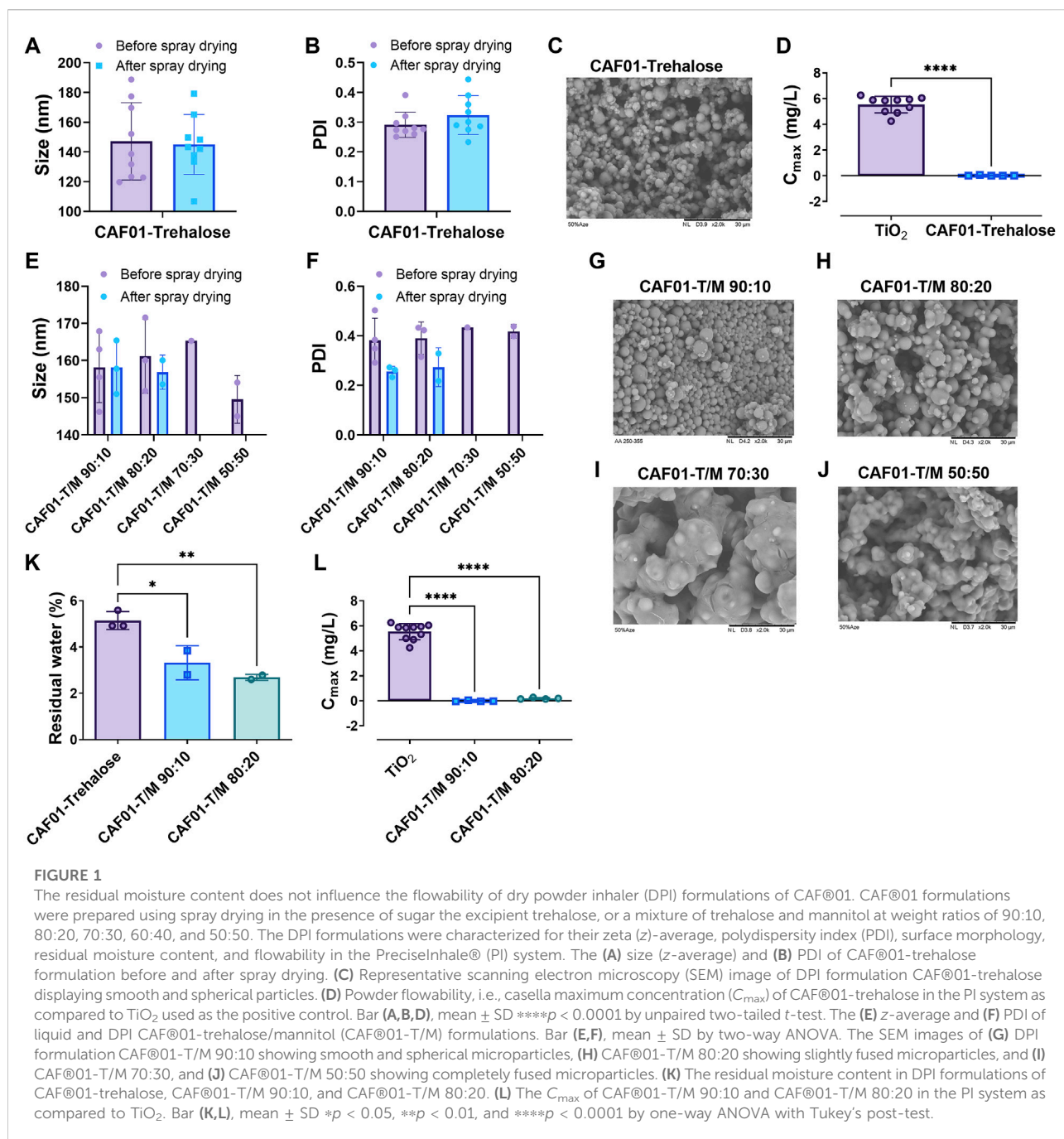
Statistical analysis

All statistical analyses of the DoE were performed using MODDE 12.0. Models were fitted with multiple linear regression. Graphing and statistical analysis were performed using GraphPad Prism v9 (Graphpad Software, La Jolla, CA, United States). The PI system data was analyzed using one- or two-way analysis of variance (ANOVA) at a 0.05 significance level, and pair-wise comparison was performed using Tukey's post-test. The residual water content was compared using one-way ANOVA at a 0.05 significance level, and pair-wise comparison was performed using Tukey's post-test. The z -average, PDI, and zeta potential data were compared using unpaired two-tailed t -test or two-way ANOVA at a 0.05 significance level, and pair-wise comparison was performed using Šidák's post-test. The *in vivo* imaging data was analyzed by two-way ANOVA at a 0.05 significance level, and pair-wise comparison was performed using Šidák's post-test. A value of $p < 0.05$ was considered statistically significant.

Results

The residual moisture content has only a slight influence on the flowability

To evaluate the influence of the type of sugar excipients used during spray drying on the flowability of the resulting powders, we prepared DPI formulations of CAF@01 with trehalose (atomizing airflow of 414 L/h) and characterized their physicochemical properties, surface morphology, and flowability in the PI system. We found that DPI formulations of CAF@01 liposomes displayed preserved physicochemical properties after spray drying using trehalose as the excipient, because no significant differences in size (Figure 1A) and PDI (Figure 1B) were observed before and after spray drying (Supplementary Table S2). The average dry powder yield was above 65% for all formulations ($68.4 \pm 3.6\%$), and the MMAD was above 6 µm (6.0 ± 3.6 µm). The surface morphology of the DPI formulations displayed smooth and spherical particles, based on SEM imaging (Figure 1C). We then evaluated the flowability (C_{max}) of the CAF@01-T DPI formulations in the PI system at the following operator settings: 120/40/4, 100/40/7, 30/12/33 (generation pressure/reset pressure/plunger



displacement) (Figure 1D). However, the flowability of these powders was very (lower than the flowability of the positive control TiO_2), and the average C_{max} of CAF@01-T DPI formulations was 0.02 mg/L, irrespective of the applied operator settings. Since trehalose has high water retention capabilities, we hypothesized: (i) that the residual moisture content of DPI CAF@01 formulations correlates with their poor flowability, and (ii) that replacing trehalose with a sugar with low hygroscopicity will improve the powder flowability. To

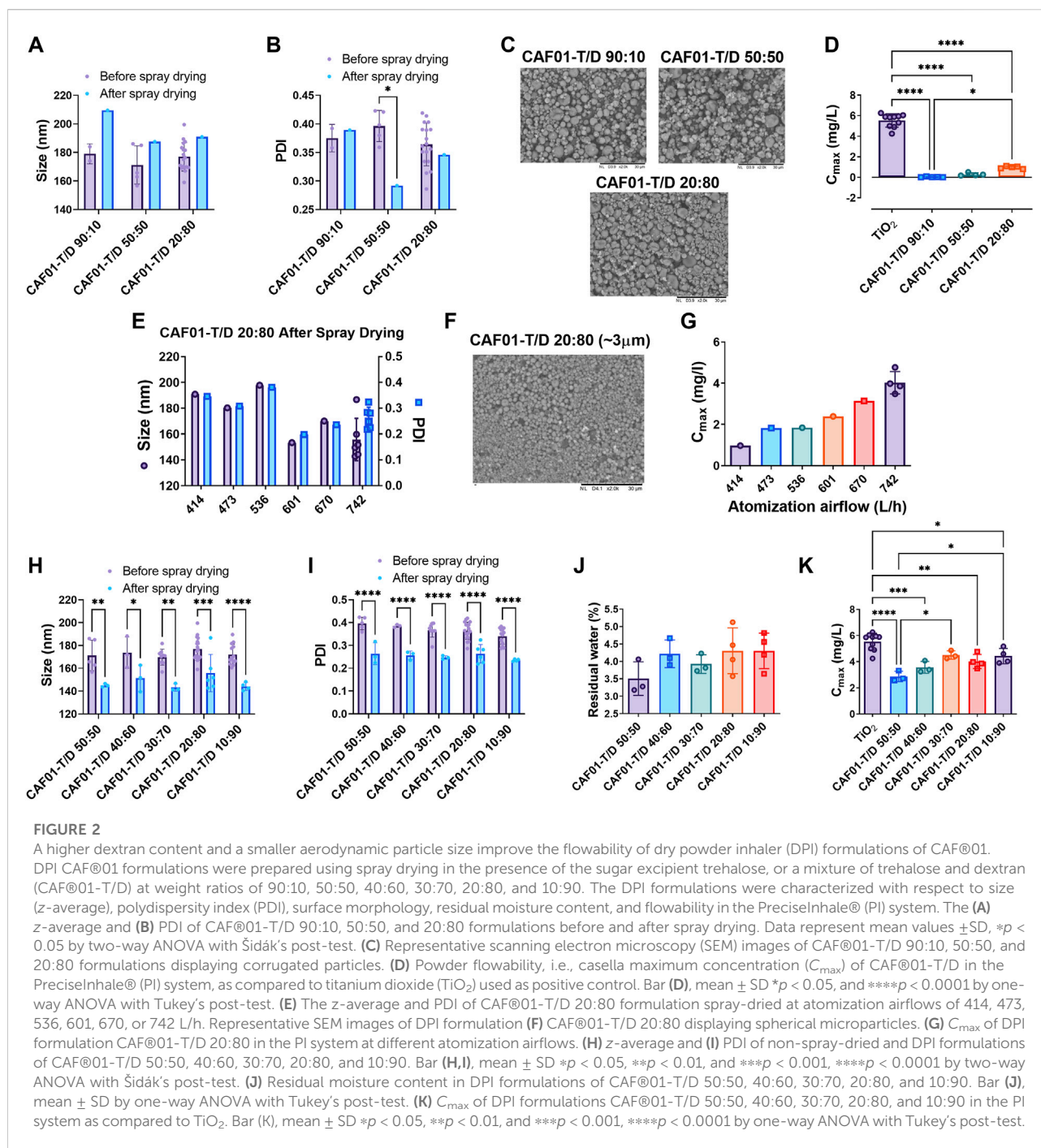
test this hypothesis, we gradually replaced trehalose with mannitol, and prepared DPI formulations of CAF@01-trehalose with 10, 20, 30, 40, and 50% (w/w) mannitol. We found that spray drying preserved the size and PDI of CAF@01-trehalose/mannitol (CAF@01-T/M) formulations, and there were no significant differences in the size (Figure 1E) and PDI (Figure 1F) before and after spray drying (Supplementary Table S2). The average dry powder yield was above 65% for CAF@01-T/M 90:10 ($69.4 \pm 12.8\%$) and CAF@01-T/M 80:20 ($67.5 \pm 4.7\%$),

but was lower for CAF@01-T/M 70:30 (~60%) and CAF@01-T/M 50:50 (~50%). The SEM images of the DPI CAF@01-T/M 90:10 formulations showed smooth and spherical microparticles with MMADs ranging from approximately 5–9 μm (Figure 1G). The DPI CAF@01-T/M 80:20 microparticles were slightly fused (Figure 1H). However, the SEM images of DPI CAF@01-T/M 70:30 (Figure 1I) and CAF@01-T/M 50:50 formulations (Figure 1J) showed completely fused particles. Based on these results, we only evaluated CAF@01-T/M 90:10 and CAF@01-T/M 80:20 formulations in further analyses. The residual moisture content of the DPI CAF@01-trehalose formulation was $5.1 \pm 0.4\%$ (Figure 1K). Indeed, we found that when increasing the mannitol content in the CAF@01-trehalose formulations, the residual moisture content was decreased to approximately 2.7% (Figure 1K). However, the lower residual moisture content did not improve the flowability of these powders, as we found a C_{max} of only 0.01 mg/L and 0.20 mg/L for CAF@01-T/M 90:10 and CAF@01-T/M 80:20, respectively (Figure 1L). Hence, these results did not support our hypothesis and suggest that the residual moisture content only slightly influence the flowability of the DPI formulations in the PI system.

Increasing the dextran content and reducing the particle size improve powder flowability

Having confirmed that residual moisture content only slightly influences the powder flowability, we next hypothesized that the type of sugar excipient used for coating the microparticles and the MMAD of particles influence their flowability in the PI system. To verify this hypothesis, we used a combination of disaccharide and polysaccharide excipients during the spray drying of CAF@01 formulations. We first prepared DPI CAF@01 formulations (CAF@01-T/D) with trehalose and an increasing content of dextran (10, 50, and 80% w/w) (atomizing airflow of 414 L/h) and characterized their physicochemical properties, surface morphology, and flowability in the PI system. We found that CAF@01-T/D liposomes prepared using different weight ratios of trehalose and dextran display mostly preserved physicochemical properties after spray drying as the sizes (Figure 2A) were not significantly different before and after spray drying (Supplementary Table S2). The PDI of only DPI formulation of CAF@01-T/D 50:50 was significantly lower than liquid CAF@01-T/D 50:50 formulation (Figure 2B). The average dry powder yield was above 65%, irrespective of the dextran content (73.5%, 70.0%, and 66.4% for CAF@01-T/D 90:10, CAF@01-T/D 50:50, and CAF@01-T/D 20:80, respectively). The MMAD of these DPI formulations was approximately 6 μm , and the average residual moisture content was 4%. The SEM images for all three formulations displayed corrugated particles with a broad size distribution (Figure 2C). We then evaluated the flowability (C_{max}) of the DPI CAF@01-T/D

formulations in the PI system at operator settings 120/40/4 (generation pressure/reset pressure/plunger displacement). The C_{max} of CAF@01-T/D 90:10 and CAF@01-T/D 50:50 was under 0.3 mg/L, while the DPI CAF@01-T/D 20:80 formulation had a significantly higher C_{max} (close to 1 mg/L) than CAF@01-T/D 90:10 and CAF@01-T/D 50:50 (Figure 2D). These results suggest that the type of sugar excipient used for coating the microparticles influence their flowability in the PI system. To evaluate the effect of particle size on the powder flowability, we prepared DPI formulations of CAF@01-T/D 20:80 by increasing the atomizing airflow from 414 L/h to 473, 536, 601, 670, and 742 L/h during spray drying. We selected the CAF@01-T/D 20:80 formulation, because it displayed the highest C_{max} among all the tested formulations (Figure 2D). Increasing the atomizing airflow did not affect the size and the PDI of the spray-dried CAF@01-T/D 20:80 (Figure 2E and Supplementary Table S3). The powder yield of the process was approximately 60%, except for DPI formulations spray-dried at an atomization airflow of 473 and 536 L/h, where the powder yield was 42.0% and 29.6%, respectively (Supplementary Table S3). The MMAD of these DPI formulations varied from 2.3–2.8 μm , and the residual moisture content was between 4.1–4.7% (Supplementary Table S3). The SEM images of DPI formulations of CAF@01-T/D 20:80 displayed spherical particles that were approximately 3 μm in size (Figure 2F and Supplementary Figure S2). When testing these DPI formulations in the PI system, we found that the flowability (C_{max}) of CAF@01-T/D 20:80 increased as the atomization airflow was increased (Figure 2G). The C_{max} of CAF@01-T/D 20:80 spray dried at an atomization airflow of 414 L/h was 0.97 mg/L, while CAF-T/D 20:80 spray dried at 742 L/h had a C_{max} of approximately 4 mg/L. However, since the MMAD of this formulation was almost similar (average 2.6 μm) at different atomizing airflows (Supplementary Table S3), another factor than particle size could be responsible for the improvement in flowability of these formulations. To verify, if a higher dextran content improves the powder flowability, we prepared DPI formulations of CAF@01-T/D using 50, 60, 70, 80, and 90% (w/w) dextran at an atomization airflow 742 L/h. We found that DPI formulations of CAF@01-T/D prepared at 50–90% (w/w) dextran display significantly lower size (Figure 2H) and PDI (Figure 2I) than non-spray dried formulations (Supplementary Table S4). The dry powder yield for all formulations was approximately 57%, and the residual water content was between 3.5 and 4.3% (Figure 2J and Supplementary Table S4). The average MMAD of these formulations was approximately 2 μm (Supplementary Table S4). SEM images also confirmed the presence of particles in this size range (Supplementary Figure S3). The aerodynamic performance of the DPI formulations was evaluated in the PI system by measuring the C_{max} . The C_{max} increased with increasing leucine content, *i.e.*, from a C_{max} at 2.8 mg/L for DPI formulations containing 50% (w/w) dextran to 3.5 mg/L for DPI formulations containing 60% (w/w) dextran and to approximately 4 and 4.5 mg/L for the DPI



formulations CAF@01-T/D 30:70 (* p < 0.05 than CAF@01-T/D 50:50), 20:80, and 10:90 (* p < 0.05 than CAF@01-T/D 50:50) (Figure 2K). The C_{max} values of the DPI formulations were significantly lower than the C_{max} of TiO₂ (approximately 5.6 mg/L), except the C_{max} of only CAF@01-T/D 30:70. Taken together, the type of sugar and the particle size influence the flowability of the DPI CAF@01 formulations in the PI system.

Identification of CAF@01 formulation with optimal powder aerosol properties

After confirming that the sugar excipients and particle size influence the flowability of the dry powders in the PI system, we used a DoE-based approach to identify the operator settings in the PI system for optimal powder flowability. The DPI formulation CAF@01-T/D 30:70 spray-dried at an atomization airflow of

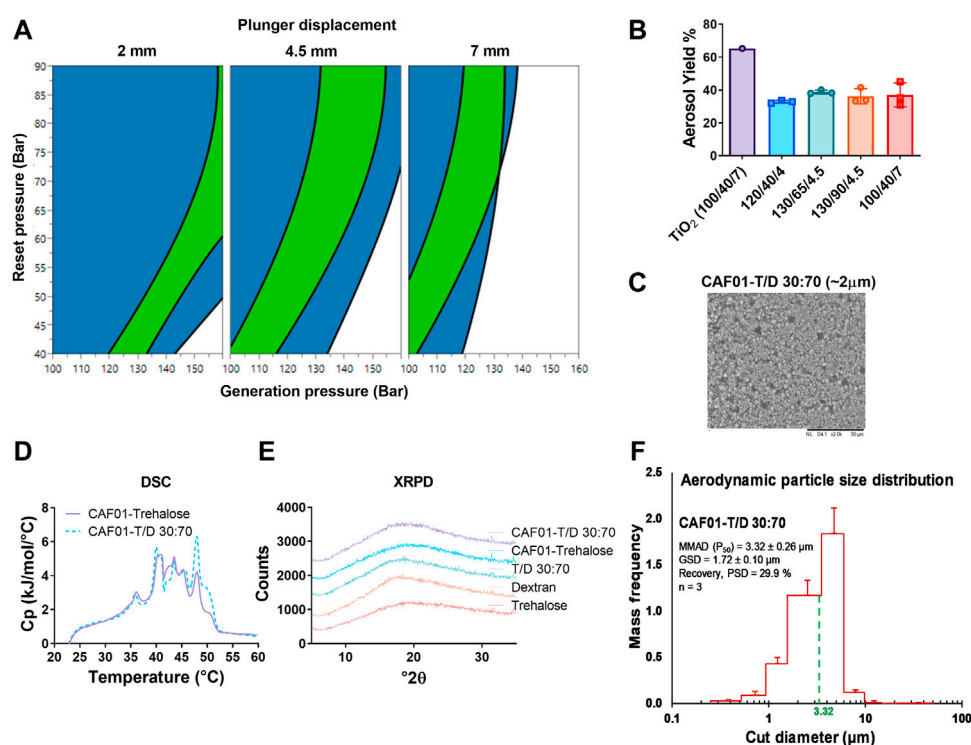


FIGURE 3

The quality-by-design approach can be used to predict powder flowability, i.e., casella maximum concentration (C_{max}) and ejected volume, and the CAF@01-trehalose/dextran 30:70 (CAF@01T/D 30:70) formulation was identified as the formulation displaying the most optimal powder aerosol properties. (A) Four dimensional sweet plot modelling of optimal operator settings in the Preciselnhale® (PI) system, i.e., plunger displacement (mm), reset pressure (bar), and generation pressure (bar). Restrictions were set for a C_{max} above 4 mg/L and an ejected volume between 75–98 ml. Color code: white (no restriction met), blue (one restriction met), and green (both restrictions met). (B) Aerosol yield of dry powder inhaler (DPI) formulation CAF@01-T/D 30:70 42L/h in the PI system at four different operator settings: 120/40/4, 130/65/4.5, 130/90/4.5, and 100/40/7 (generation pressure/reset pressure/plunger displacement), $n = 3$, mean \pm SD. (C) Representative scanning electron microscopy (SEM) image of CAF@01-T/D 30:70 formulation displaying spherical particles. (D) Representative differential scanning calorimetry (DSC) thermograph (first scan) of reconstituted DPI CAF@01-trehalose (black solid) and CAF@01-T/D 30:70 (red dots) formulations. (E) Representative X-ray powder diffraction (XRPD) patterns of CAF@01-T/D 30:70 (red), CAF@01-trehalose (black), trehalose/dextran 30:70 (grey), dextran (blue), and trehalose (green). The patterns have been displaced on the y-axis for clarity. (F) Aerodynamic particle size distribution of DPI CAF@01-T/D 30:70 formulation measured in the PI system connected to a 9-stage Marple Cascade Impactor. The mass median aerodynamic diameter (MMAD) was estimated to be around $3.53 \pm 0.31 \mu\text{m}$ (dotted green line), $n = 3$, data represents mean values \pm SD.

742 L/h was used for DoE, because it displayed the highest C_{max} and the lowest standard deviation (Figure 2K). For the experimental design, C_{max} was restricted to be higher than 4 mg/L, as this was the lowest obtained value with the DPI CAF@01-T/D 30:70 formulation at an atomization airflow of 742 L/h. The ejected volume was restricted between 75 and 98 ml, which is within the range recommended for optimal *in vivo* performance of powders in the PI system by the manufacturer. For C_{max} , a good model fit was obtained with a validity of approximately 0.5, and the ejected volume resulted in a very good model with an R^2 , Q^2 , and reproducibility close to 1 (Supplementary Figure S4). A 4-D sweet spot plot was constructed with plunger displacement on the outer axis, while reset pressure and generation pressure were depicted on the inner x- and y-axes, respectively (Figure 3A). The reset pressure allowed for a larger operating space, while the generation pressure seemed

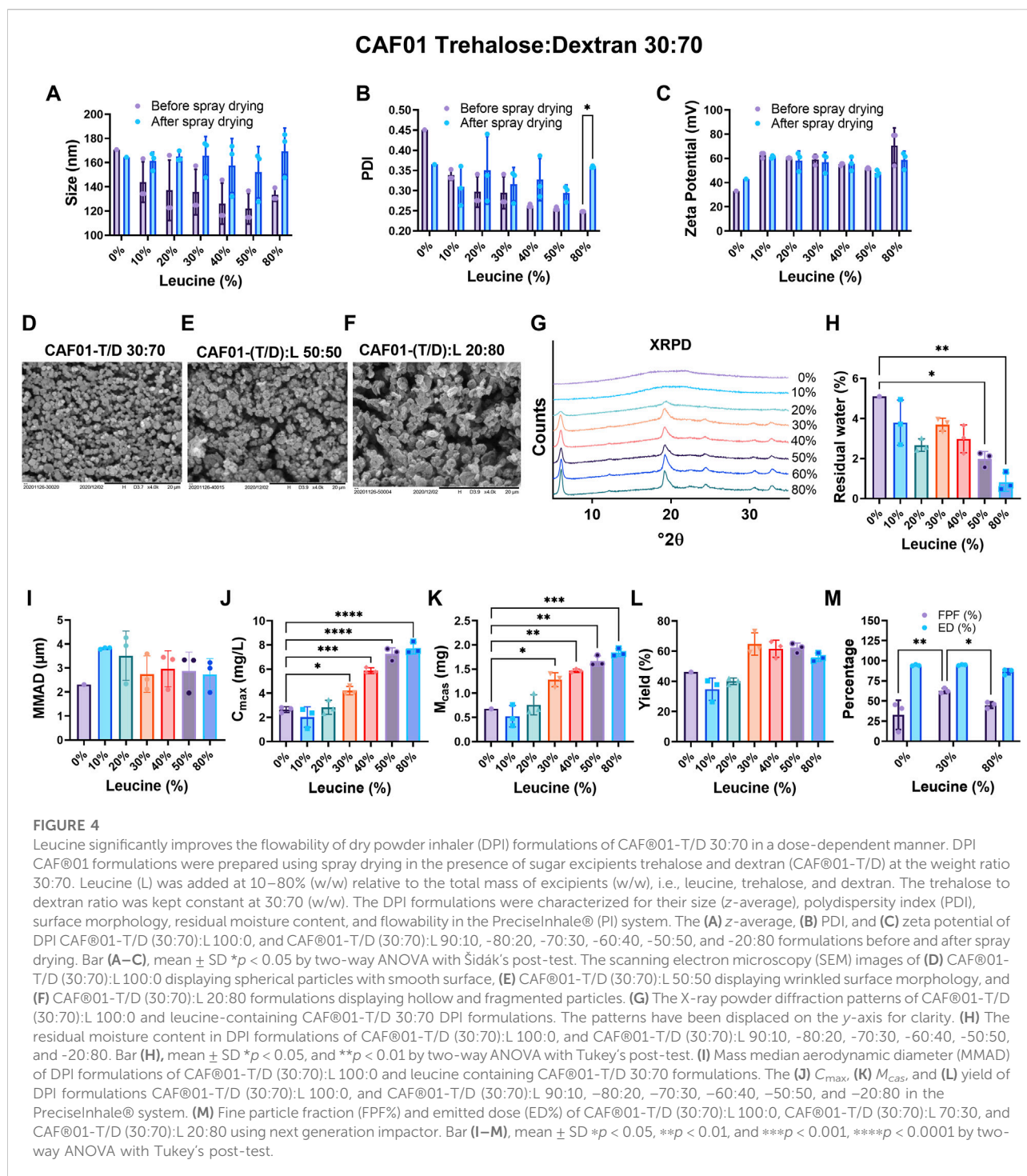
to have a restricted range to reach the optimal responses, which depended on the plunger displacement. For instance, at plunger displacements at low (2 mm) and high level (7 mm), the generation pressure was around 120–160 bar and 100–130 bar, respectively. When the plunger displacement was adjusted to center level, i.e., 4.5 mm, the range of generation pressure was wider, i.e., between 100 and 150 bar to get the optimal responses (Figure 3A). We then measured the aerosol yield of the DPI CAF@01-T/D 30:70 formulation in the PI system to determine its suitability for further *in vivo* evaluation. Based on DoE results for the highest C_{max} (Supplementary Table S5), four different operator settings were used to measure the aerosol yield: 120/40/4, 130/65/4.5, 130/90/4.5, and 100/40/7 (generation pressure/reset pressure/plunger displacement). These operator settings resulted in a C_{max} between 4.5–5.0 mg/ml and an ejected volume of between 70–96 mg/ml (Supplementary Table S5). The aerosol

yield was 33, 39, 36 and 37% at operator settings 120/40/4, 130/65/4.5, 130/90/4.5, and 100/40/7, respectively (Figure 3B). The SEM images of DPI CAF@01-T/D 30:70 formulation showed spherical particles (Figure 3C). We then evaluated the thermotropic phase behaviour of reconstituted DPI CAF@01-trehalose and CAF@01-T/D 30:70 formulations using DSC (Figure 3D). Two main interconnected transition peaks were observed at approximately 40–41 °C and 43–46 °C. Moreover, in the first scan, two endothermic peaks at 35–36 °C and 48–49 °C were evident (Figure 3D), but these peaks disappeared in the second and third DSC scans (Supplementary Figure S5). As suggested previously, this phenomenon is because of incomplete hydration of the lipid bilayer in the first scan (Ingvarsson et al., 2013a). We then calculated the T_m , $T_{1/2}$ and ΔH_m of these formulations, but found no significant difference between the formulations (Supplementary Table S6). XRPD was used to determine the solid state of the DPI CAF@01-T/D 30:70 formulation. As controls, we used CAF@01-trehalose and stabilizing sugars, including trehalose, dextran, and a mixture of trehalose/dextran at 30:70 (w/w). All spray-dried sugars and DPI liposome formulations showed a halo pattern typical for amorphous structures (Figure 3E). We also analyzed the PSD of DPI CAF@01-T/D 30:70 formulation in the PI system connected to a 9-stage Cascade Impactor (Figure 3F). The powder recovery was 27.7% and the MMAD was $3.53 \pm 0.31 \mu\text{m}$. The MMAD measured with the PI system was higher than that calculated using the APS, which was $1.99 \pm 0.23 \mu\text{m}$. The particle size of DPI CAF@01-T/D 30:70 was also calculated based on ImageJ analysis of SEM image, and a particle size of $1.77 \pm 0.17 \mu\text{m}$ ($n = 3$) was determined. The zeta potential for the CAF@01-T/D 30:70 formulation measured in trehalose/dextran 30:70 solution was found to be consistent before and after spray drying (Supplementary Table S7). The zeta potential of CAF@01-T/D 30:70 was very similar to the zeta potential of the CAF@01-T formulation before and after reconstitution of the powders. Using Tris buffer (pH 7.4), we also determined similar zeta potential for DPI CAF@01-T/D 30:70 and CAF@01-trehalose formulations as the non-spray-dried CAF@01 formulation. Overall, the DPI CAF@01-T/D 30:70 formulation displayed optimal powder aerosol properties.

Leucine improves the flowability of DPI formulations

Following identification of the optimal PI process parameters and trehalose:dextran ratio (w/w) for preparing DPI formulation of CAF@01, we hypothesized that spray drying in the presence of crystalline amino acid leucine, which is a known dispersion enhancer, will form an anti-adherent shell on the surface of particles that will further enhance the powder flowability (Mangal et al., 2015; Xu et al., 2022a). To test this hypothesis, we systematically incorporated leucine at weight ratios of 10%–

80% (w/w) during spray drying of CAF@01 keeping the trehalose and dextran weight ratio constant at 30:70. We found that the size (Figure 4A) and PDI (Figure 4B) of CAF@01-T/D 30:70 liposomes decreased as the leucine content was increased. However, the PDI of DPI CAF@01-T/D 30:70 containing 80% (w/w) leucine was significantly higher after spray drying (Figure 4B). The zeta potential increased upon incorporation of leucine in the sugar matrix, but it remained constant for all leucine weight ratios (Figure 4C). Including leucine during spray drying influenced the surface morphology of CAF@01-T/D 30:70 liposomes in a leucine dose-dependent manner. CAF@01-T/D (30:70) displayed spherical particles with a smooth surface (Figure 4D), while the powder containing 50% leucine displayed a wrinkled surface morphology (Figure 4E). Including 80% leucine resulted in hollow and fragmented particles (Figure 4F). Leucine containing DPI formulation of CAF@01 at 10%–40% (w/w) ratios transformed from particles with a spherical morphology to a wrinkled surface appearance (Supplementary Figures S6A–D). In XRPD analysis, DPI formulations without leucine and with 10% leucine showed a halo pattern, which is typical for amorphous structures (Figure 4G). However, formulations containing >20% leucine (w/w) showed a crystalline structure. Liposomes containing 20% leucine (w/w) displayed only two $[6.00^\circ, 19.04^\circ 2(\theta)]$ of the six diffraction peaks observed for DPI formulations containing 30%–80% leucine (w/w). Moreover, the peak intensities were dependent on the mass ratio of leucine to saccharides (trehalose and dextran). The residual moisture content in the DPI formulations was dependent on the mass percentage of leucine in the formulations, and the moisture content decreased as the leucine content was increased (Figure 4H). The DPI formulations CAF@01-T/D (30:70):L 50:50 and CAF@01-T/D (30:70):L 20:80 displayed a significantly lower residual moisture content than CAF@01-T/D (30:70):L 100:0. The MMAD of all leucine-containing DPI formulations were similar, but were not significantly larger than the MMAD of DPI formulations without leucine (Figure 4I). To evaluate the effect of leucine on powder flowability, these formulations were tested in the PI system. It was observed that the C_{max} (Figure 4J) and M_{cas} (Figure 4K) increased as the leucine content (w/w) was increased in the DPI formulations. However, the aerosol yield (%) of the DPI formulations in the PI system increased following incorporation of $\geq 30\%$ leucine (w/w) and remained constant until 80% leucine (w/w) (Figure 4L). Following these observations, three DPI formulations of CAF@01-T/D (30:70) containing 30% and 80% leucine or without leucine were tested for aerosolization behavior using the NGI (Figure 4M and Supplementary Figures S6E–G). All three formulations had a very high ED, and approximately 95% of the DPI formulation was released during aerosolization, and no DPI formulation was left in the capsules. However, the FPF was significantly higher for the DPI formulation CAF@01-T/D (30:70):L 70:30, as compared to other formulations. We also evaluated the DDA content in the



DPI formulations CAF@01-T/D (30:70):L 100:0, -60:40, -50:50, and -20:80 before and after spray drying using HPLC. The HPLC chromatograms displayed one distinct peak corresponding to DDA eluting after 6.45 min (Supplementary Figure S6H). The HPLC chromatograms of the non-spray dried and DPI

formulations of CAF@01-T/D (30:70):L also showed a peak eluting at 6.45 min corresponding to DDA. Although the percentage of DDA recovery (Supplementary Figure S6I) and concentration of DDA (Supplementary Figure S6J) in DPI CAF@01-T/D (30:70):L 100:0, -60:40, -50:50, and -20:

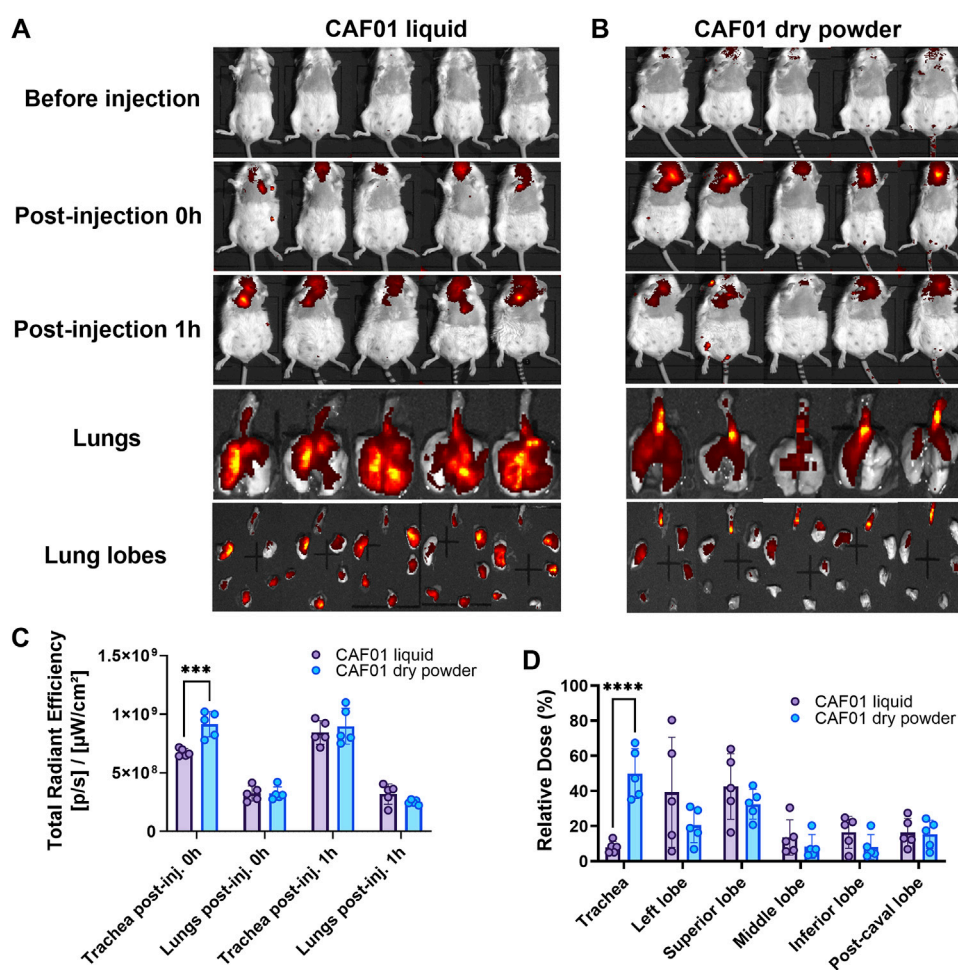


FIGURE 5

Dry powder inhaler (DPI) CAF@01-Trehalose/Dextran (30:70):Leucine 70:30 formulation distributes almost similarly in lung lobes as the non-spray-dried CAF@01-Trehalose/Dextran (30:70):Leucine 70:30. Xenolight™ DiR-labeled DPI CAF@01 formulations were prepared using spray drying of CAF@01 in the presence of sugar excipients trehalose and dextran at the weight ratio 30:70, and leucine was added at 30% (w/w) relative to the total mass of excipients (w/w), i.e., leucine, trehalose, and dextran. Female BALB/c mice were dosed intrapulmonary with either 50 µL liquid Xenolight™ DiR-labeled CAF@01-(T/D):L 70:30 formulation using PennCentury MicroSprayer® Aerosolizer or 1 mg Xenolight™ DiR-labeled DPI formulation CAF@01-(T/D):L 70:30 using the PennCentury Dry Powder Insufflator™. Representative IVIS images of mice before injection, immediately post-injection, and 1 h post-injection, intact lungs, and dissected lungs showing deposition of (A) liquid and (B) DPI formulation. (C) Total radiant efficiency in the trachea and the five lung lobes (together). (D) Relative percentage of dose in the trachea and the individual lung lobes. Bar, mean ± SD (n = 5). ***p < 0.001 via two-way ANOVA with Šidák post-test.

80 formulations were slightly lower after spray drying, no significant differences were observed for these values between non-spray dried and DPI formulations.

Pulmonary distribution of aerosols of DPI CAF@01-Trehalose/Dextran (30:70): Leucine 70:30 formulation

Based on the above results, the DPI formulation of CAF@01 co-spray-dried with 30% (w/w) Leu and 70% (w/w) T:D (30:70, w/w) was selected as the lead formulation for imaging

the *in vivo* pulmonary biodistribution. Xenolight™ DiR-labelled CAF@01, as liquid dispersions or DPI formulations, was administered intrapulmonary into the lungs of mice, and the animals were imaged using IVIS imaging. The inhaler retention of the DPI formulation in the DP-4M insufflator was determined from the delivered dose. The retention of the DPI formulation was 24.7% for 1 mg and 29.1% for 2 mg powder loading, and the first air puff in the DP-4M insufflator was the most efficient one (Supplementary Figure S6K). In our recent study using siRNA-loaded lipid-polymer hybrid nanoparticles, we observed that using 2 mg powder dose, a large amount of powder flew out of the mouth of the animals during dosing (Xu et al., 2022a).

Therefore, in this study, we selected a dose of 1 mg powder for imaging. Following pulmonary administration, a fluorescent signal was observed for both liquid and DPI formulation of Xenolight™ DiR-labelled CAF@01 in mice lungs (Figures 5A,B). Based on the images, liquid formulation distributed evenly in the lungs and different lung lobes, as compared to the DPI formulation. For quantitative analysis, a ROI was placed around the trachea, lungs, and the different lung lobes (Figure 5C). The total fluorescence intensity in the trachea, as well as in the lungs of the mice dosed with DPI formulation, was similar to the intensities in mice receiving liquid formulation. However, immediately after administration (0 h), the signal in the trachea in the mice dosed with dry powders was significantly higher than the signal in mice receiving the liquid formulation (Figure 5C). The total fluorescence intensity in the lungs was approximately one log lower than that in trachea at both 0 and 1 h post-administration. Upon dissecting the lungs into individual lung lobes, bright fluorescent spots were detected in all lung lobes for the liquid formulation (Figure 5A), as compared to the DPI formulation, and some lung lobes did not emit any fluorescent signal (Figure 5B). The biodistribution of the formulations was further assessed by calculating the relative percentage of the dose in the trachea and the individual lung lobes of mice (Figure 5D). Corresponding to the images, a slightly higher relative dose of liquid formulation was observed in the lung lobes, as compared to the dose of DPI formulations. For the DPI formulation, a significantly higher dose was retained in the trachea, as compared to liquid formulation.

Discussion

The liposome-based CAF@01 has been tested as a vaccine carrier and adjuvant system for subunit antigens in multiple clinical studies (Roman et al., 2013; van Dissel et al., 2014; Abraham et al., 2019; Dejon-Agobe et al., 2019). We have previously shown that reconstituted DPI formulations of CAF@01 adjuvanted with the TB subunit antigen H56 maintain immunogenicity of H56 when compared with the non-spray dried vaccine formulation (Thakur et al., 2018b). With the long-term objective to develop a thermostable self-administrable H56-based vaccine against TB, we optimized the design and dosing of DPI formulations of CAF@01 without H56 for pulmonary immunization in this study. We manufactured DPI formulations of CAF@01 using trehalose alone or in combination with either mannitol or dextran or dextran and leucine as stabilizing excipients. We then characterized the physicochemical, morphological, solid-state, and aerosol properties of DPI formulations. We used a QbD approach to identify optimal process parameters associated with the flowability of dry powders in the PI system. We finally investigated the uptake and distribution in lungs of the

most optimal DPI formulation of CAF@01 following pulmonary administration in mice.

Our previous results have demonstrated that trehalose, when used as a stabilizer during spray drying, maintains the physicochemical properties of CAF@01 upon rehydration (Ingvarsson et al., 2013b). In addition, reconstituted DPI formulations of CAF@01 spray-dried with trehalose, when combined with H56, had preserved adjuvant activity *in vivo* (Ingvarsson et al., 2013a). We also showed that reconstituted DPI formulations of H56/CAF@01-trehalose vaccine had preserved T cell and humoral immune responses as the non-spray dried H56/CAF@01 vaccine (Thakur et al., 2018b). To evaluate the aerosol properties and lung uptake of DPI formulations of CAF@01, we therefore tested formulations prepared with trehalose alone and combinations of trehalose with mannitol, dextran, and/or leucine. We found that the liquid vaccine formulations prepared with different sugar solutions displayed similar size and PDI as the CAF@01 liposomes usually prepared with tris buffer (pH 7.4). A comparison of the liquid formulations with the reconstituted DPI formulations showed a slight decrease in size and PDI after spray drying, which supports our previous results (Ingvarsson et al., 2013a). This effect was observed with trehalose, trehalose/mannitol, and trehalose/dextran mixtures, as well as at all atomization airflows used during spray drying. The reduction of liposome size after spray drying has been previously described in the literature (Wessman et al., 2010). This finding was explained by a reorganization of the lipid bilayer due to an osmotically driven invagination of the liposomes that causes unilamellar liposomes to shrink in size, which become bi-lamellar as a consequence of the drying process (Wessman et al., 2010). However, reconstituted DPI formulations of CAF@01-T/D (90:10), CAF@01-T/D (50:50), and CAF@01-T/D (20:80) spray-dried at an atomization airflow of 414 L/h showed small aggregations, and their size was slightly higher than the liquid formulations. The DPI formulations of CAF@01-T/D (30:70) prepared with leucine displayed non-significantly higher size and PDI with increasing concentrations of leucine. Prior studies have reported an increased particle size of liposomes after spray drying with L-leucine and lactose (Mangal et al., 2015; Thiyagarajan et al., 2021) due to aggregation in the dissolved microparticle samples (Thiyagarajan et al., 2021). In our recent study with DPI formulations of lipid-polymer hybrid nanoparticles spray-dried with a combination of trehalose, dextran and leucine, we also observed a slight increase in the particle size of nanoparticles after spray drying (Xu et al., 2022a). This is in contrast to other reports, where the reduced particle size with increased leucine content was primarily due to reduced droplet size during the spray drying, caused by reduced interfacial tension of the droplets due to accumulation of L-leucine at the air-liquid interface, caused by its relative hydrophobicity (Rabbani and Seville, 2005; Cruz et al., 2011). The slight increase in particle size of DPI formulations of CAF@01 liposomes could be due to crystalline leucine being combined with amorphous sugars

during spray drying. The zeta potential of CAF@01-T/D 30:70 liquid and reconstituted DPI formulations was similar as previously measured for CAF@01 liquid formulations showing positively charged liposomes (Hamborg et al., 2014). However, a significant decrease in the zeta potential was measured in sugar solution, as compared to measurements performed in Tris buffer (pH 7.4). This decrease was because of the ionization state of the sugars and differences in the pH of the buffers. The addition of leucine did not influence the liposome charge as all the DPI formulations of CAF@01-T/D (30:70) prepared with leucine had similar zeta potential before and after spray drying.

Spray drying CAF@01 with trehalose resulted in powders with a residual moisture content of approximately 5%, which was higher than previously reported (3.2%–3.7%) (Ingvarsson et al., 2013a). This difference can be a result of different ambient air humidity during spray drying. Trehalose is one of the most commonly used sugars as stabilizer during spray drying because of its high glass transition temperature (T_g) of $\sim 117^\circ\text{C}$ that allows the maintenance of an amorphous glassy matrix for stabilizing the liposomes. However, it is well-known that trehalose is highly hygroscopic and is responsible for higher moisture content in the powder formulations (Jain and Roy, 2009). The DPI formulations of CAF@01-T displayed poor flowability in the PI system, as compared to TiO_2 , and agglomerates of the DPI formulation were found after exposure in the PI system. Due to the high amount of moisture in the DPI formulations, which influences their stability and flow properties, CAF@01 was stabilized during spray drying with mixtures of trehalose and mannitol with the objective to reduce the water content and to increase the flowability in the PI system. Our previous results show that DPI formulations of CAF@01-M liposomes had very low residual moisture content of 0.5%–0.7% (Ingvarsson et al., 2013a). The difference in the moisture uptake between trehalose and mannitol is because amorphous structures such as trehalose have a higher tendency to absorb water, whereas mannitol, which is crystalline, has a low residual moisture content (Mihriyan et al., 2004). However, crystallization of mannitol reduces the stability and when spray drying with mannitol, the use of excipients that inhibit its crystallization may be useful in extending the utility of mannitol as a stabilizer (Costantino et al., 1998). The DPI CAF@01-T/M formulations showed a lower moisture content, compared with CAF@01-trehalose, but CAF@01-T/M had poor flowability in the PI system, suggesting that moisture is not the only parameter that affects the flowability of the DPI formulations containing trehalose and mannitol. However, for leucine-modified DPI formulations of CAF@01-T/D (30:70), the residual moisture content decreased when the leucine content was increased, which is accompanied by a corresponding increase in the powder flowability in the PI system. Leucine has a known anti-hygroscopic effect on powders obtained after spray drying (Li et al., 2017; Xu et al., 2022a) and minimizes moisture-induced deterioration in the aerosol performance of powders (Li et al., 2016). The

moisture protective mechanism of leucine has been attributed to the enrichment of leucine on the surface of microparticles (Li et al., 2016). The high crystallinity of leucine on the surface of microparticles has also been associated with very low water uptake, thereby reducing interaction between particle surface and moisture (Li et al., 2016). We have also observed a similar phenomenon in our recent study with DPI formulations of siRNA-loaded lipid-polymer hybrid nanoparticles (Xu et al., 2022a).

Dextran (6 kDa) was selected as stabilizer with trehalose because combinations of a polysaccharide and disaccharide can produce structures that are more rigid and have a higher coating density (Tonnis et al., 2015). In addition, previous studies have reported that mixtures of trehalose and dextran increase the T_g of formulations and improve their storage stability (Allison et al., 2000; Tonnis et al., 2015). A freeze-dried influenza vaccine formulated with a mixture of trehalose/dextran was found to have physicochemical characteristics suitable for inhalation and had excellent stabilization properties (Murugappan et al., 2013). Our DPI formulations prepared with trehalose and dextran displayed a higher C_{max} in the PI system than formulations prepared with only trehalose or trehalose and mannitol. However, no significant differences were found in neither particle size (MMAD) nor residual moisture content between formulations spray-dried with or without dextran. These results suggest the importance of type of sugars in the stabilization of liposomes during spray drying. Furthermore, DPI formulations prepared with an increasing concentration of dextran showed higher flowability. An increment in the rigidity of the structures and a higher coating density of the microparticles with dextran could be associated with the higher C_{max} and consequently a higher flowability (Tonnis et al., 2015). It has been shown that more porous particles with higher surface areas, which result from the formulations containing the highest dextran concentrations, may show better aerodynamic properties (Kadota et al., 2019).

Deep lung delivery of particles is dependent on the MMAD, and particles with an MMAD between 1 and 5 μm are optimal to reach alveolar region, while particles between 5–10 μm are trapped in the upper respiratory tract (Blank et al., 2011; Sou et al., 2011). Using a QbD approach, we have previously shown that the atomization airflow has the largest influence on the particle MMAD, which is characterized by an inverse relationship (Ingvarsson et al., 2013b). All DPI formulations of CAF@01, irrespective of the type of stabilizing sugar, prepared at an atomization airflow of 414 L/h showed an MMAD higher than 5 μm and a corresponding low flowability in the PI system. Upon increasing the atomization airflow (473, 536, 601, 670 and 742 L/h) during spray drying of the CAF@01-T/D 20:80 formulation, particles with almost similar MMAD were produced (approximately 2.5 μm). As previously described, the larger energy input to atomize the feed dispersion into smaller droplets results in reduced particle size (Maltesen et al., 2008)

explaining the negative effect of atomization airflow on MMAD. This explanation supports the MMAD reduction measured when the atomization airflow was increased from 414 to 473 L/h, but atomization airflows higher than 473 L/h did not further reduce the particle size. The reason for the similar MMAD is that there are other factors during spray drying that control the particle size. Probably, the limit for the droplet size was reached with the conditions used during spray drying. Furthermore, the MMAD is also highly influenced by the feedstock concentration (Maltesen et al., 2008; Ingvarsson et al., 2013b). Due to high trehalose/dextran concentration, a higher atomization airflow would not have affected the particle size. This phenomenon could possibly explain the increase in MMAD of CAF@01-T/D (30:70) particles containing leucine. The effect of atomization airflow on the flowability of the DPI formulations was less evident. The atomization airflow showed a clear positive influence on the C_{max} . However, the MMAD and the residual moisture content, which are parameters that influence the flowability of the powders, did not change at higher atomization airflows. However, the atomization airflow could affect other powder characteristics, e.g., particle density, that influences the aerosolization properties (Seville et al., 2007). Further studies are required to investigate the influence of the different physicochemical properties including particle density on the flowability of DPI formulations.

The surface morphology of DPI particles can also affect their aerosolization performance. It has been described that surface corrugation produces a considerable improvement in aerosolization of DPI formulations with otherwise similar properties (particle size, density and moisture) (Chew and Chan, 2001; Chew and Chan, 2002; Xu et al., 2022a). Surface corrugation enhances the flowability of powders, because the distance between particles is increased, and the total particle area accessible for interaction is decreased (Chew and Chan, 2001; Chew et al., 2005). Another advantage of corrugated particles is that the choice of inhaler and the airflow become less critical (Chew and Chan, 2001). We also observed that DPI CAF@01-T/D particles that displayed a corrugated surface had a higher flowability in the PI system, as compared to CAF@01-T and CAF@01-T/M formulations that displayed smooth spherical particles. The inclusion of dextran and use of a higher atomization airflow could increase the degree of surface corrugation of the DPI formulations and in turn their flowability. A relatively small degree of surface corrugation is sufficient to accomplish a considerable improvement in the aerosol performance of the powders (Chew et al., 2005). Incorporation of leucine changed the morphology of the microparticles from spherical particles with a smooth surface to corrugated particles at 50% (w/w) and to hollow and fragmented (doughnut) particles at >50% leucine (w/w). These doughnut-like particles suggest the formation of hollow and collapsed particles, which have a higher aerosol performance than dense particles with a smooth surface (Xu et al., 2022a).

Moreover, the hydrophobic nature of the outer leucine shell resists solid bridge formation between particles and hence reduces interparticle forces and improves powder flowability (Sou et al., 2013; Mangal et al., 2018).

XRPD analyses showed an amorphous pattern for DPI formulations of CAF@01-Trehalose and CAF@01-T/D 30:70. Trehalose with a high T_g of $\sim 117^\circ\text{C}$ allows the maintenance of an amorphous glassy matrix for stabilizing the liposome-based adjuvants and subunit proteins. Previously, both the process stability and the storage stability of subunit Hepatitis B virus vaccine was improved by incorporating the antigen in an amorphous matrix of a combination of dextran and trehalose (Tonnis et al., 2014a). Moreover, the thermogram of reconstituted DPI CAF@01-T/D 30:70 formulation showed similar thermal events as previously reported for CAF@01 liquid formulation (Davidsen et al., 2005; Hamborg et al., 2014). Therefore, sugars are not affecting the thermodynamic parameters of CAF@01 liposomes. The thermograms of the formulations, which displayed interconnected peaks at $40\text{--}41^\circ\text{C}$ and $43\text{--}46^\circ\text{C}$, suggest a heterogeneous distribution of DDA and TDB resulting in microdomains rich in one of the lipids (Davidsen et al., 2005). Upon incorporation of $\geq 20\%$ leucine in CAF@01-T/D 30:70 formulations, diffraction peaks characteristic of crystalline structures were observed. It is known that during spray drying, leucine molecules tend to accumulate at the surface of droplets with their hydrophobic part facing the air phase and it crystallizes encircling the droplet with a crystalline hydrophobic outer-shell (Simon et al., 2016) and form a hollow particle (Kaewjan and Srichana, 2016). Using leucine in combination with trehalose and dextran, we have recently shown that leucine forms a crystalline outer shell around the microparticles (Xu et al., 2022a). This outer shell of leucine then shrinks due to continuous evaporation of the solvent, and wrinkled particles are formed, which along with the hydrophobic nature of the leucine outer shell resist interparticle interaction and improve flowability (Sou et al., 2013). Hence, the microparticles of DPI CAF@01 with an amorphous trehalose/dextran matrix and a crystalline leucine shell stabilize the liposomes, and ensure aerosol properties suitable for inhalation (Xu et al., 2022a).

The PI system has been used for delivering DPI formulations *in vivo* and allows controlled delivery of aerosols for pulmonary administration (Fioni et al., 2018; Lexmond et al., 2018). Furthermore, the PI system can be used to measure the aerosol concentration and breathing pattern in real-time. However, it is important to study the influence of different process parameters (*i.e.* PI system settings) on the aerosolization of DPI formulations. Instead of using the conventional one-factor-at-a-time approach, we varied and tested three process parameters (generation pressure, reset pressure, and plunger displacement) in the PI system at the same time and identified the sweet spot with the best aerosol performance of the powders. Leucine, being an independent

formulation parameter in this case, will not have any influence on the process parameters of the PI system. Therefore, once we identified the most optimal settings of the instrument, we incorporated leucine as a formulation parameter to further enhance the aerosol performance of the powders. Generation pressure, reset pressure, and plunger displacement in the PI system control the ejected volume and the C_{max} of the particles. Based on QbD using DoE, the ejected volume, which is not affected by the powder formulation, was shown to have a model reproducibility close to 1. Therefore, the ejected volume can be accurately predicted depending on the selected PI system settings. On the other hand, the C_{max} had a lower model reproducibility as a result of some variability in the measurements, but was acceptable. As previously reported, the C_{max} variability can be explained by spontaneous variations in the dose deposition in the PI system (Malmlof et al., 2019). The QbD model in our study suggested that generation pressure and plunger displacement have the strongest influence on ejected volume and C_{max} but it remains unclear how these two settings are affecting the responses.

Although, the PI system can be used for delivery of aerosols in rats and guinea pigs, respirable aerosol exposure in mice with a high dose, *i.e.*, 1–2 mg, remains a challenge, as we have recently reported (Xu et al., 2022a). Our lung phantom exposure results with DPI CAF@01-T/D 30:70 formulation confirm this observation (Supplementary Material S1.3 and Supplementary Figure S7). We therefore used the PennCentury Dry Powder Insufflator™, which can be used to deliver 1–2 mg respiratory aerosol into mice lungs. The PennCentury Dry Powder Insufflator™ has been reported to deposit the majority of the DPI formulation in the large airways and not in the deep lungs (Tonnis et al., 2014b). We also observed that a significant fraction of the delivered DPI formulation of CAF@01-(T/D):L 70:30 remained in the trachea as compared to the liquid formulation. However, no significant differences in distribution of DPI formulation of CAF@01-(T/D):L 70:30 was observed in the lung lobes as compared to the liquid formulation. Using 2 mg loaded dose of powders of lipid-polymer hybrid nanoparticles, we did not observe any tracheal deposition (Xu et al., 2022a). Therefore, administration of respiratory aerosols using the PennCentury Dry Powder Insufflator™ may not be the most optimal method, but it can certainly be used for proof-of-concept studies to understand pulmonary deposition and distribution of DPI formulations *in vivo* and this technique requires further optimization. Notably, the intrapulmonary administration of DPI formulations in mice differs from the intrapulmonary delivery of drugs in humans. Intrapulmonary drug delivery in humans can be achieved through inhalation aerosols (also known as metered dose inhalers (or MDIs) and inhalation powders or DPIs. DPIs differ from MDIs in that they are breath-actuated (breath-dose coordination is unnecessary) and easier to use. Both DPIs and MDIs are based on patient inspiratory flow to ensure correct inhalation and deposition of drugs in the lungs. However, in mice, intrapulmonary delivery can

only be performed under deep anesthesia where the person administering the drug has to coordinate drug instillation or insufflation with the breathing of the animal. The site of deposition of a DPI vaccine formulation has considerable impact on the ensuing immunogenicity. It has been shown that for a DPI-based subunit influenza vaccine, comparable immune responses were induced upon trachea/central airways or deep lung targeting (Tomar et al., 2019). However, for a DPI-based subunit hepatitis B vaccine, immune responses were only induced after deep lung deposition but not by trachea/central airways deposition (Tomar et al., 2019). Since the DPI formulation of CAF@01-(T/D):L 70:30 distributes both in the trachea/central airways and deep lungs, we believe that the site of deposition will be of minor relevance for vaccine immunogenicity, but this remains to be tested.

The DPI formulations of CAF@01-(T/D):L 70:30 were prepared without H56. We have previously demonstrated that DPI formulations of CAF01® prepared with (Thakur et al., 2018b) or without H56 (Ingvarsson et al., 2013a) did not affect their immunogenic or adjuvant function, respectively. Therefore, we do not expect that including H56 will affect the functional properties of CAF@01-(T/D):L 70:30 formulation. Moreover, the low temperature conditions used during spray drying can preserve the function of co-formulated H56 protein in its native state. Using similar formulation and spray drying process parameters, we have recently shown the preserved function (Xu et al., 2022a) and long-term stability of siRNA-containing nanoparticles (Xu et al., 2022b). Based on these results, we can speculate that the stability and the delivery properties of DPI formulations of CAF@01-(T/D):L 70:30 will not be affected upon co-formulation with H56. However, the functional properties of DPI formulations of H56/CAF@01-(T/D):L 70:30 remain to be verified.

Overall, DPI formulations of CAF@01-(T/D):L 70:30 exhibited physicochemical and solid-state properties optimal for aerosolization and distributed in lung lobes after pulmonary administration. Our results demonstrate that the type of sugar and amount (w/w) of amino acid coating used as stabilizer during spray drying affects the physicochemical properties and aerosol performance of the DPI formulations. Using a DoE-based approach, we identified the most optimal process parameters in the PI system that determine the flowability of the aerosols. We also show that incorporation of crystalline shell-forming leucine with the amorphous sugars trehalose and dextran during spray drying significantly increases the particle flowability, as compared to the formulations containing only trehalose and dextran. Pulmonary administration of the most optimal DPI formulation CAF@01-(T/D):L 70:30 resulted in distribution of formulation to all the lung lobes. Based on these properties, we believe that DPI formulation of CAF@01-(T/D):L 70:30 can be used for evaluating the prophylactic efficacy of co-administered subunit antigen H56 in animal models of TB challenge following administration of respiratory aerosols. The prophylactic efficacy of this DPI formulation can be compared with the non-spray dried vaccine formulation that we have shown to induce robust H56-specific immune responses in the lungs.

Data availability statement

The original contributions presented in the study are included in the article/[Supplementary Material](#), further inquiries can be directed to the corresponding authors.

Ethics statement

The animal study was reviewed and approved by the Danish National Experiment Inspectorate under permit 2016-15-0201-01026.

Author contributions

AT and CF designed the study. AT, YX, GC-G, SF, and FR performed the laboratory work and analyzed the data. AT, FR, and CF interpreted the data. AT, YX, and GC-G drafted the manuscript. AT, PG, PA, DC, and CF provided scientific input throughout the study period and drafting of the manuscript. CF acquired the funding.

Funding

This work was supported by The Danish Council for Independent Research, Technology and Production Sciences (grant number DFF-4184-00422).

Acknowledgments

We thank Ewa Selg and Carl-Olof Sjöberg for technical inputs during the PreciseInhale® experiments. We are grateful to the animal technicians at the Department of Drug Design and Pharmacology, University of Copenhagen for their animal

References

- Abraham, S., Juel, H. B., Bang, P., Cheeseman, H. M., Dohn, R. B., Cole, T., et al. (2019). Safety and immunogenicity of the chlamydia vaccine candidate CTH522 adjuvanted with CAF01 liposomes or aluminium hydroxide: A first-in-human, randomised, double-blind, placebo-controlled, phase 1 trial. *Lancet. Infect. Dis.* 19, 1091–1100. doi:10.1016/S1473-3099(19)30279-8
- Agger, E. M., Rosenkrands, I., Hansen, J., Brahimi, K., Vandahl, B. S., Aagaard, C., et al. (2008). Cationic liposomes formulated with synthetic mycobacterial cordfactor (CAF01): A versatile adjuvant for vaccines with different immunological requirements. *PLoS One* 3 (9), e3116. doi:10.1371/journal.pone.0003116
- Ajmera, A., and Scherliess, R. (2014). Stabilisation of proteins via mixtures of amino acids during spray drying. *Int. J. Pharm.* 463 (1), 98–107. doi:10.1016/j.ijpharm.2014.01.002
- Allison, S. D., Manning, M. C., Randolph, T. W., Middleton, K., Davis, A., and Carpenter, J. F. (2000). Optimization of storage stability of lyophilized actin using combinations of disaccharides and dextran. *J. Pharm. Sci.* 89 (2), 199–214. doi:10.1002/(SICI)1520-6017(200002)89:2<199::AID-JPS7>3.0.CO;2-B
- Blank, F., Stumbles, P., and von Garnier, C. (2011). Opportunities and challenges of the pulmonary route for vaccination. *Expert Opin. Drug Deliv.* 8 (5), 547–563. doi:10.1517/17425247.2011.565326
- Chew, N. Y., and Chan, H. K. (2002). The role of particle properties in pharmaceutical powder inhalation formulations. *J. Aerosol Med.* 15 (3), 325–330. doi:10.1089/089426802760292672
- Chew, N. Y., and Chan, H. K. (2001). Use of solid corrugated particles to enhance powder aerosol performance. *Pharm. Res.* 18 (11), 1570–1577. doi:10.1023/a:1013082531394
- Chew, N. Y., Tang, P., Chan, H. K., and Raper, J. A. (2005). How much particle surface corrugation is sufficient to improve aerosol performance of powders? *Pharm. Res.* 22 (1), 148–152. doi:10.1007/s11095-004-9020-4
- Christensen, D., Christensen, J. P., Korsholm, K. S., Isling, L. K., Erneholm, K., Thomsen, A. R., et al. (2017). Seasonal influenza split vaccines confer partial cross-protection against heterologous influenza virus in ferrets when combined

husbandry services. We acknowledge the Drug Research Academy Graduate Programme in Pharmaceutical Sciences, University of Copenhagen, for funding the Small-Scale Powder Disperser. Novo Nordisk, Denmark, has kindly supplied the Aerodynamic Particle Sizer Spectrometer 3321 and the Next Generation Pharmaceutical Impactor.

Conflict of interest

Author PG is employed by Inhalation Sciences Sweden AB. Author DC is employed by Statens Serum Institut, a nonprofit government research facility, of which the CAF® adjuvants are proprietary products.

The remaining authors declare that the research was conducted in the absence of any commercial or financial relationships that could be construed as a potential conflict of interest.

Publisher's note

All claims expressed in this article are solely those of the authors and do not necessarily represent those of their affiliated organizations, or those of the publisher, the editors and the reviewers. Any product that may be evaluated in this article, or claim that may be made by its manufacturer, is not guaranteed or endorsed by the publisher.

Supplementary material

The Supplementary Material for this article can be found online at: <https://www.frontiersin.org/articles/10.3389/fddev.2022.973599/full#supplementary-material>

- with the CAF01 adjuvant. *Front. Immunol.* 8, 1928. doi:10.3389/fimmu.2017.01928
- Costantino, H. R., Andya, J. D., Nguyen, P. A., Dasovich, N., Sweeney, T. D., Shire, S. J., et al. (1998). Effect of mannitol crystallization on the stability and aerosol performance of a spray-dried pharmaceutical protein, recombinant humanized anti-IgE monoclonal antibody. *J. Pharm. Sci.* 87 (11), 1406–1411. doi:10.1021/js9800679
- Cruz, L., Fattal, E., Tasso, L., Freitas, G. C., Carregaro, A. B., Guterres, S. S., et al. (2011). Formulation and *in vivo* evaluation of sodium alendronate spray-dried microparticles intended for lung delivery. *J. Control. Release* 152 (3), 370–375. doi:10.1016/j.jconrel.2011.02.030
- Davidson, J., Rosenkrands, I., Christensen, D., Vangala, A., Kirby, D., Perrie, Y., et al. (2005). Characterization of cationic liposomes based on dimethyldioctadecylammonium and synthetic cord factor from *M. tuberculosis* (trehalose 6, 6'-dibehenate)-a novel adjuvant inducing both strong CMI and antibody responses. *Biochim. Biophys. Acta* 1718 (1-2), 22–31. doi:10.1016/j.bbame.2005.10.011
- Dejon-Agobe, J. C., Ateba-Ngoa, U., Lalremruata, A., Homoet, A., Engelhorn, J., Nouatin, O. P., et al. (2019). Controlled human malaria infection of healthy adults with lifelong malaria exposure to assess safety, immunogenicity, and efficacy of the asexual blood stage malaria vaccine candidate GMZ2. *Clin. Infect. Dis.* 69 (8), 1377–1384. doi:10.1093/cid/ciy1087
- Del Giudice, G., Rappuoli, R., and Didierlaurent, A. M. (2018). Correlates of adjuvanticity: A review on adjuvants in licensed vaccines. *Semin. Immunol.* 39, 14–21. doi:10.1016/j.smim.2018.05.001
- Fioni, A., Selg, E., Cenacchi, V., Acevedo, F., Brogin, G., Gerde, P., et al. (2018). Investigation of lung pharmacokinetic of the novel PDE4 inhibitor CHF6001 in preclinical models: Evaluation of the PreciseInhale technology. *J. Aerosol Med. Pulm. Drug Deliv.* 31 (1), 61–70. doi:10.1089/jamp.2017.1369
- Fomsgaard, A., Karlsson, I., Gram, G., Schou, C., Tang, S., Bang, P., et al. (2011). Development and preclinical safety evaluation of a new therapeutic HIV-1 vaccine based on 18 T-cell minimal epitope peptides applying a novel cationic adjuvant CAF01. *Vaccine* 29 (40), 7067–7074. doi:10.1016/j.vaccine.2011.07.025
- Gerde, P., Ewing, P., Lastbom, L., Ryrfeldt, A., Waher, J., and Liden, G. (2004). A novel method to aerosolize powder for short inhalation exposures at high concentrations: Isolated rat lungs exposed to respirable diesel soot. *Inhal. Toxicol.* 16 (1), 45–52. doi:10.1080/08958370490258381
- Ghaemmaghamian, Z., Zarghami, R., Walker, G., O'Reilly, E., and Ziaee, A. (2022). Stabilizing vaccines via drying: Quality by design considerations. *Adv. Drug Deliv. Rev.* 187, 114313. doi:10.1016/j.addr.2022.114313
- Gomez, M., and Vehring, R. (2022). Spray drying and particle engineering in dosage form design for global vaccines. *J. Aerosol Med. Pulm. Drug Deliv.* 35, 121–138. doi:10.1089/jamp.2021.0056
- Henriksen-Lacey, M., Christensen, D., Bramwell, V. W., Lindenstrom, T., Agger, E. M., Andersen, P., et al. (2010). Liposomal cationic charge and antigen adsorption are important properties for the efficient deposition of antigen at the injection site and ability of the vaccine to induce a CMI response. *J. Control. Release* 145 (2), 102–108. doi:10.1016/j.jconrel.2010.03.027
- Hamborg, M., Rose, F., Jorgensen, L., Bjorklund, K., Pedersen, H. B., Christensen, D., et al. (2014). Elucidating the mechanisms of protein antigen adsorption to the CAF/NAF liposomal vaccine adjuvant systems: Effect of charge, fluidity and antigen-to-lipid ratio. *Biochim. Biophys. Acta* 1838 (8), 2001–2010. doi:10.1016/j.bbame.2014.04.013
- Ingvarsson, P. T., Schmidt, S. T., Christensen, D., Larsen, N. B., Hinrichs, W. L., Andersen, P., et al. (2013). Designing CAF-adjuvanted dry powder vaccines: Spray drying preserves the adjuvant activity of CAF01. *J. Control. Release* 167 (3), 256–264. doi:10.1016/j.jconrel.2013.01.031
- Ingvarsson, P. T., Yang, M., Mulvad, H., Nielsen, H. M., Rantanen, J., and Foged, C. (2013). Engineering of an inhalable DDA/TDB liposomal adjuvant: A quality-by-design approach towards optimization of the spray drying process. *Pharm. Res.* 30 (11), 2772–2784. doi:10.1007/s11095-013-1096-2
- Iwasaki, A., and Omer, S. B. (2020). Why and how vaccines work. *Cell.* 183 (2), 290–295. doi:10.1016/j.cell.2020.09.040
- Jain, N. K., and Roy, I. (2009). Effect of trehalose on protein structure. *Protein Sci.* 18 (1), 24–36. doi:10.1002/pro.3
- Kadota, K., Yanagawa, Y., Tachikawa, T., Deki, Y., Uchiyama, H., Shirakawa, Y., et al. (2019). Development of porous particles using dextran as an excipient for enhanced deep lung delivery of rifampicin. *Int. J. Pharm.* 555, 280–290. doi:10.1016/j.ijpharm.2018.11.055
- Kaewjan, K., and Srichana, T. (2016). Nano spray-dried pyrazinamide-L-leucine dry powders, physical properties and feasibility used as dry powder aerosols. *Pharm. Dev. Technol.* 21 (1), 68–75. doi:10.3109/10837450.2014.971373
- Lapiente, D., Fuchs, J., Willar, J., Vieira Antao, A., Eberlein, V., Uhlig, N., et al. (2021). Protective mucosal immunity against SARS-CoV-2 after heterologous systemic prime-mucosal boost immunization. *Nat. Commun.* 12 (1), 6871. doi:10.1038/s41467-021-27063-4
- Lexmond, A. J., Keir, S., Terakosolphan, W., Page, C. P., and Forbes, B. (2018). A novel method for studying airway hyperresponsiveness in allergic Guinea pigs *in vivo* using the PreciseInhale system for delivery of dry powder aerosols. *Drug Deliv. Transl. Res.* 8, 760–769. doi:10.1007/s13346-018-0490-z
- Li, L., Leung, S. S. Y., Gengenbach, T., Yu, J., Gao, G. F., Tang, P., et al. (2017). Investigation of L-leucine in reducing the moisture-induced deterioration of spray-dried salbutamol sulfate powder for inhalation. *Int. J. Pharm.* 530 (1-2), 30–39. doi:10.1016/j.ijpharm.2017.07.033
- Li, L., Sun, S., Parumasivam, T., Denman, J. A., Gengenbach, T., Tang, P., et al. (2016). L-Leucine as an excipient against moisture on *in vitro* aerosolization performances of highly hygroscopic spray-dried powders. *Eur. J. Pharm. Biopharm.* 102, 132–141. doi:10.1016/j.ejpb.2016.02.010
- Lokras, A., Foged, C., and Thakur, A. (2021). Engineering of solid dosage forms of siRNA-loaded lipidoid-polymer hybrid nanoparticles using a quality-by-design approach. *Methods Mol. Biol.* 2282, 137–157. doi:10.1007/978-1-0716-1298-9_9
- Malmlof, M., Nowenwik, M., Meelich, K., Radberg, I., Selg, E., Burns, J., et al. (2019). Effect of particle deposition density of dry powders on the results produced by an *in vitro* test system simulating dissolution- and absorption rates in the lungs. *Eur. J. Pharm. Biopharm.* 139, 213–223. doi:10.1016/j.ejpb.2019.03.005
- Maltesen, M. J., Bjerregaard, S., Hovgaard, L., Havelund, S., and van de Weert, M. (2008). Quality by design - spray drying of insulin intended for inhalation. *Eur. J. Pharm. Biopharm.* 70 (3), 828–838. doi:10.1016/j.ejpb.2008.07.015
- Mangal, S., Meiser, F., Tan, G., Gengenbach, T., Denman, J., Rowles, M. R., et al. (2015). Relationship between surface concentration of L-leucine and bulk powder properties in spray dried formulations. *Eur. J. Pharm. Biopharm.* 94, 160–169. doi:10.1016/j.ejpb.2015.04.035
- Mangal, S., Nie, H., Xu, R., Guo, R., Cavallaro, A., Zemlyanov, D., et al. (2018). Physico-chemical properties, aerosolization and dissolution of Co-spray dried azithromycin particles with L-leucine for inhalation. *Pharm. Res.* 35 (2), 28. doi:10.1007/s11095-017-2334-9
- Mensink, M. A., Frijlink, H. W., van der Voort Maarschalk, K., and Hinrichs, W. L. (2017). How sugars protect proteins in the solid state and during drying (review): Mechanisms of stabilization in relation to stress conditions. *Eur. J. Pharm. Biopharm.* 114, 288–295. doi:10.1016/j.ejpb.2017.01.024
- Mihriyan, A., Llagostera, A. P., Karmhag, R., Stromme, M., and Ek, R. (2004). Moisture sorption by cellulose powders of varying crystallinity. *Int. J. Pharm.* 269 (2), 433–442. doi:10.1016/j.ijpharm.2003.09.030
- Murugappan, S., Patil, H. P., Kanojia, G., ter Veer, W., Meijerhof, T., Frijlink, H. W., et al. (2013). Physical and immunogenic stability of spray freeze-dried influenza vaccine powder for pulmonary delivery: Comparison of inulin, dextran, or a mixture of dextran and trehalose as protectants. *Eur. J. Pharm. Biopharm.* 85 (3), 716–725. doi:10.1016/j.ejpb.2013.07.018
- Neuzil, K. M., Bresee, J. S., de la Hoz, F., Johansen, K., Karron, R. A., Krishnan, A., et al. (2017). Data and product needs for influenza immunization programs in low- and middle-income countries: Rationale and main conclusions of the WHO preferred product characteristics for next-generation influenza vaccines. *Vaccine* 35 (43), 5734–5737. doi:10.1016/j.vaccine.2017.08.088
- Perdomo, C., Zedler, U., Kuhl, A. A., Lozza, L., Saikali, P., Sander, L. E., et al. (2016). Mucosal BCG vaccination induces protective lung-resident memory T cell populations against tuberculosis. *MBio* 7 (6), e01686–16. doi:10.1128/mBio.01686-16
- Rabbani, N. R., and Seville, P. C. (2005). The influence of formulation components on the aerosolisation properties of spray-dried powders. *J. Control. Release* 110 (1), 130–140. doi:10.1016/j.jconrel.2005.09.004
- Remy, V., Zollner, Y., and Heckmann, U. (2015). Vaccination: The cornerstone of an efficient healthcare system. *J. Mark. Access Health Policy* 3, 27041. doi:10.3402/jmahp.v3.27041
- Roman, V. R., Jensen, K. J., Jensen, S. S., Leo-Hansen, C., Jespersen, S., da Silva Te, D., et al. (2013). Therapeutic vaccination using cationic liposome-adjuvanted HIV type 1 peptides representing HLA-supertype-restricted subdominant T cell epitopes: Safety, immunogenicity, and feasibility in Guinea-bissau. *AIDS Res. Hum. Retroviruses* 29 (11), 1504–1512. doi:10.1089/AID.2013.0076
- Schoenen, H., Bodendorfer, B., Hitchens, K., Manzanero, S., Werninghaus, K., Nimmerjahn, F., et al. (2010). Cutting edge: Mincle is essential for recognition and adjuvanticity of the mycobacterial cord factor and its synthetic analog trehalose-dibehenate. *J. Immunol.* 184 (6), 2756–2760. doi:10.4049/jimmunol.0904013
- Schrager, L. K., Chandrasekaran, P., Fritzell, B. H., Hatherill, M., Lambert, P. H., McShane, H., et al. (2018). WHO preferred product characteristics for new vaccines against tuberculosis. *Lancet. Infect. Dis.* 18 (8), 828–829. doi:10.1016/S1473-3099(18)30421-3

- Selg, E., Ewing, P., Acevedo, F., Sjoberg, C. O., Ryrfeldt, A., and Gerde, P. (2013). Dry powder inhalation exposures of the endotracheally intubated rat lung, *ex vivo* and *in vivo*: The pulmonary pharmacokinetics of fluticasone furoate. *J. Aerosol Med. Pulm. Drug Deliv.* 26 (4), 181–189. doi:10.1089/jamp.2012.0971
- Seville, P. C., Li, H. Y., and Learoyd, T. P. (2007). Spray-dried powders for pulmonary drug delivery. *Crit. Rev. Ther. Drug Carr. Syst.* 24 (4), 307–360. doi:10.1615/critrevtherdrugcarriersyst.v24.i4.10
- Simon, A., Amaro, M. I., Cabral, L. M., Healy, A. M., and de Sousa, V. P. (2016). Development of a novel dry powder inhalation formulation for the delivery of rivastigmine hydrogen tartrate. *Int. J. Pharm.* 501 (1–2), 124–138. doi:10.1016/j.ijpharm.2016.01.066
- Sou, T., Kaminskas, L. M., Nguyen, T. H., Carlberg, R., McIntosh, M. P., and Morton, D. A. (2013). The effect of amino acid excipients on morphology and solid-state properties of multi-component spray-dried formulations for pulmonary delivery of biomacromolecules. *Eur. J. Pharm. Biopharm.* 83 (2), 234–243. doi:10.1016/j.ejpb.2012.10.015
- Sou, T., Meeusen, E. N., de Veer, M., Morton, D. A., Kaminskas, L. M., and McIntosh, M. P. (2011). New developments in dry powder pulmonary vaccine delivery. *Trends Biotechnol.* 29 (4), 191–198. doi:10.1016/j.tibtech.2010.12.009
- Thakur, A., Ingvarsson, P. T., Schmidt, S. T., Rose, F., Andersen, P., Christensen, D., et al. (2018). Immunological and physical evaluation of the multistage tuberculosis subunit vaccine candidate H56/CAF01 formulated as a spray-dried powder. *Vaccine* 36 (23), 3331–3339. doi:10.1016/j.vaccine.2018.04.055
- Thakur, A., Rodriguez-Rodriguez, C., Saatchi, K., Rose, F., Esposito, T., Nosrati, Z., et al. (2018). Dual-isotope SPECT/CT imaging of the tuberculosis subunit vaccine H56/CAF01: Induction of strong systemic and mucosal IgA and T-cell responses in mice upon subcutaneous prime and intrapulmonary boost immunization. *Front. Immunol.* 9, 2825. doi:10.3389/fimmu.2018.02825
- Thiyagarajan, D., Huck, B., Nothdurft, B., Koch, M., Rudolph, D., Rutschmann, M., et al. (2021). Spray-dried lactose-leucine microparticles for pulmonary delivery of antimycobacterial nanopharmaceuticals. *Drug Deliv. Transl. Res.* 11 (4), 1766–1778. doi:10.1007/s13346-021-01011-7
- Tomar, J., Tonnis, W. F., Patil, H. P., de Boer, A. H., Hagedoorn, P., Vanbever, R., et al. (2019). Pulmonary immunization: Deposition site is of minor relevance for influenza vaccination but deep lung deposition is crucial for Hepatitis B vaccination. *Acta Pharm. Sin. B* 9 (6), 1231–1240. doi:10.1016/j.apsb.2019.05.003
- Tonnis, W. F., Amorij, J. P., Vreeman, M. A., Frijlink, H. W., Kersten, G. F., and Hinrichs, W. L. (2014). Improved storage stability and immunogenicity of Hepatitis B vaccine after spray-freeze drying in presence of sugars. *Eur. J. Pharm. Sci.* 55, 36–45. doi:10.1016/j.ejps.2014.01.005
- Tonnis, W. F., Bagerman, M., Weij, M., Sjollem, J., Frijlink, H. W., Hinrichs, W. L., et al. (2014). A novel aerosol generator for homogenous distribution of powder over the lungs after pulmonary administration to small laboratory animals. *Eur. J. Pharm. Biopharm.* 88 (3), 1056–1063. doi:10.1016/j.ejpb.2014.10.011
- Tonnis, W. F., Mensink, M. A., de Jager, A., van der Voort Maarschalk, K., Frijlink, H. W., and Hinrichs, W. L. (2015). Size and molecular flexibility of sugars determine the storage stability of freeze-dried proteins. *Mol. Pharm.* 12 (3), 684–694. doi:10.1021/mp500423z
- van Dissel, J. T., Joosten, S. A., Hoff, S. T., Soonawala, D., Prins, C., Hokey, D. A., et al. (2014). A novel liposomal adjuvant system, CAF01, promotes long-lived Mycobacterium tuberculosis-specific T-cell responses in human. *Vaccine* 32 (52), 7098–7107. doi:10.1016/j.vaccine.2014.10.036
- Wehring, R. (2008). Pharmaceutical particle engineering via spray drying. *Pharm. Res.* 25 (5), 999–1022. doi:10.1007/s11095-007-9475-1
- Vierboom, M. P. M., Dijkman, K., Sombroek, C. C., Hofman, S. O., Boot, C., Vervenne, R. A. W., et al. (2021). Stronger induction of trained immunity by mucosal BCG or MTBVAC vaccination compared to standard intradermal vaccination. *Cell. Rep. Med.* 2 (1), 100185. doi:10.1016/j.xcrm.2020.100185
- Wang, W. (2000). Lyophilization and development of solid protein pharmaceuticals. *Int. J. Pharm.* 203 (1–2), 1–60. doi:10.1016/s0378-5173(00)00423-3
- Wern, J. E., Sorensen, M. R., Olsen, A. W., Andersen, P., and Follmann, F. (2017). Simultaneous subcutaneous and intranasal administration of a CAF01-adjuvanted Chlamydia vaccine elicits elevated IgA and protective Th1/Th17 responses in the genital tract. *Front. Immunol.* 8, 569. doi:10.3389/fimmu.2017.00569
- Werninghaus, K., Babiak, A., Gross, O., Holscher, C., Dietrich, H., Agger, E. M., et al. (2009). Adjuvanticity of a synthetic cord factor analogue for subunit Mycobacterium tuberculosis vaccination requires FcRgamma-Syk-Card9-dependent innate immune activation. *J. Exp. Med.* 206 (1), 89–97. doi:10.1084/jem.20081445
- Wessman, P., Edwards, K., and Mahlin, D. (2010). Structural effects caused by spray- and freeze-drying of liposomes and bilayer disks. *J. Pharm. Sci.* 99, 2032–2048. doi:10.1002/jps.21972
- WHO. WHO target product profiles for COVID-19 vaccines. Revised version April 2022. (2022).
- Xu, Y., Harinck, L., Lokras, A. G., Gerde, P., Selg, E., Sjoberg, C. O., et al. (2022). Leucine improves the aerosol performance of dry powder inhaler formulations of siRNA-loaded nanoparticles. *Int. J. Pharm.* 621, 121758. doi:10.1016/j.ijpharm.2022.121758
- Xu, Y., Turan, E. T., Shi, Z., Franzzyk, H., Thakur, A., and Foged, C. (2022). Inhalable composite microparticles containing siRNA-loaded lipid-polymer hybrid nanoparticles: Saccharides and leucine preserve aerosol performance and long-term physical stability. *Front. Drug Deliv.* 2 (945459), 1–15. doi:10.3389/fddev.2022.945459